Pergamon

Bioorganic & Medicinal Chemistry 10 (2002) 779–801

BIOORGANIC & MEDICINAL CHEMISTRY

Novel Potent 5-HT_3 Receptor Ligands Based on the Pyrrolidone Structure: Synthesis, Biological Evaluation, and Computational Rationalization of the Ligand–Receptor Interaction Modalities

Andrea Cappelli,[a,*] Maurizio Anzini,[b] Salvatore Vomero,[a] Laura Mennuni,[c] Francesco Makovec,[c] Edith Doucet,[d] Michel Hamon,[d] M.Cristina Menziani,[e] Pier G. De Benedetti,[e] Gianluca Giorgi,[f] Carla Ghelardini[g] and Simona Collina[h]

[a]*Dipartimento Farmaco Chimico Tecnologico, Università di Siena, Via A. Moro, 53100 Siena, Italy*
[b]*Dipartimento di Scienze Farmacobiologiche, Università di Catanzaro "Magna Graecia", Complesso Ninì Barbieri, 88021 Roccelletta di Borgia, Catanzaro, Italy*
[c]*Rotta Research Laboratorium S.p.A., Via Valosa di Sopra 7, 20052 Monza, Italy*
[d]*Neuropsychopharmacologie Moléculaire, Cellulaire et Fonctionnelle, INSERM U. 288, Faculté de Médecine Pitié-Salpêtrière, 91, Boulevard de l'Hôpital, 75634 Paris Cedex 13, France*
[e]*Dipartimento di Chimica, Università degli Studi di Modena e Reggio Emilia, Via Campi 183, 41100 Modena, Italy*
[f]*Centro Interdipartimentale di Analisi e Determinazioni Strutturali, Università di Siena, Via A. Moro, 53100 Siena, Italy*
[g]*Dipartimento di Farmacologia Preclinica e Clinica "Mario Aiazzi Mancini", Università degli Studi di Firenze, Viale Pieraccini 6, 50139 Firenze, Italy*
[h]*Dipartimento di Chimica Farmaceutica, Università di Pavia, Via Taramelli 12, 27100 Pavia, Italy*

Received 9 July 2001; accepted 20 September 2001

Abstract—Novel conformationally constrained derivatives of classical 5-HT_3 receptor antagonists were designed and synthesized with the aim of probing the central 5-HT_3 receptor recognition site in a systematic way. The newly-synthesized compounds were tested for their potential ability to inhibit [^{3}H]granisetron specific binding to 5-HT_3 receptor in rat cortical membranes. These studies revealed subnanomolar affinity in some of the compounds under study. The most potent ligand in this series was found to be quinuclidine derivative (*S*)-**7i**, which showed an affinity comparable with that of the reference ligand granisetron. The potential 5-HT_3 agonist/antagonist activity of some selected compounds was assessed in vitro on the 5-HT_3 receptor-dependent [^{14}C]guanidinium uptake in NG 108-15 cells. Both of the tropane derivatives tested in this functional assay (**7a** and **9a**) showed antagonist properties, while the quinuclidine derivatives studied [the enantiomers of compounds **7i**, **8g**, and **9g**, and compound (*R*)-**8h**] showed a full range of intrinsic efficacies. Therefore, the functional behavior of these 5-HT_3 receptor ligands appears to be affected by the structural features of both the azabicyclo moiety and the heteroaromatic portion. In agreement with the data obtained on NG 108-15 cells, investigations on the 5-HT_3 receptor-dependent Bezold–Jarisch reflex in urethane-anaesthetized rats confirmed the 5-HT_3 receptor antagonist properties of compounds **7a** and (*S*)-**7i** showing for these compounds ID_{50} values of 2.8 and 181 μg/kg, respectively. Finally, compounds **7a**, (*S*)-**7i** and **9a** (at the doses of 0.01, 1.0, and 0.01 mg/kg ip, respectively) prevented scopolamine-induced amnesia in the mouse passive avoidance test suggestive of a potential usefulness in cognitive disorders for these compounds. Qualitative and quantitative structure–affinity relationship studies were carried out by means of theoretical descriptors derived on a single structure and ad-hoc defined size and shape descriptors (indirect approach). The results showed to be useful in capturing information relevant to ligand–receptor interaction. Additional information derived by the analysis of the energy minimized 3-D structures of the ligand–receptor complexes (direct approach) suggested interesting mechanistic and methodological considerations on the binding mode multiplicity at the 5-HT_3 receptors and on the degree of tolerance allowed in the alignment of molecules for the indirect approach, respectively.

*Corresponding author. Tel.: +39-0577-234-320; fax: +39-0577-234-333; e-mail: cappelli@unisi.it

0968-0896/02/$ - see front matter
PII: S0968-0896(01)00332-7

Introduction

Among the wide variety of serotonin (5-hydroxytryptamine, 5-HT) receptors so far identified, the 5-HT_3 receptor subtype stands alone. This receptor is a ligand-gated ion channel that mediates fast depolarizing responses and is apparently selective for the monovalent cations Na^+ and K^+.[1] Current evidence indicates that the 5-HT_3 receptor exhibits the pentameric structure characteristic of the ligand-gated ion channels (LGICs) such as nicotinic acetylcholine (nACh), glycine, and type A γ-aminobutyric acid ($GABA_A$) receptors.[2] These receptors are constituted by assemblies of five hetero- (nAChR, glycineR, and $GABA_AR$) or homo-subunits (5-HT_3R) surrounding a central transbilayer pore. Each subunit has a large N-terminal extracellular domain, four putative transmembrane segments and an intracellular domain. Composite ligand binding sites, conserved throughout the Cys-loop receptor superfamily, are located at the interface of two subunits formed by residues belonging to two components.[1] The transition to an open, active state of the nAChR seems to be favoured by the occupation of two agonist binding sites, but a ligand–receptor complex with a stoichiometry of 1:1 seems to be sufficient for the homomeric 5-HT_3R function.[3]

The three-dimensional (3-D) structure of 5-HT_3 receptor has not been resolved at the atomic level. However, the great amount of information emerged from electron microscopy data,[4] photoaffinity labelling, and site-directed mutagenesis studies[5] on the member of this receptor family was recently used to derive a 3-D model of the 5-HT_3 receptor extracellular domain.[6]

The development of selective 5-HT_3 receptor antagonists has received a great deal of attention in recent years and the therapeutic role of ondansetron (**1**), granisetron (BRL 43694, **2**), and tropisetron (**3**) as antiemetic drugs has been clearly established (Chart 1). Furthermore, preclinical studies suggested that 5-HT_3 receptor antagonists might be clinically useful in a number of situations. These include depressive, cognitive, and psychotic disorders, drug and alcohol abuse, treatment of pain and irritable bowel syndrome.[7]

Our group has been involved for several years in the development of 5-HT_3 receptor ligands based on the arylpiperazine structure, and we recently proposed a pharmacophoric model for the interaction of arylpiperazine ligands **4** with their receptor.[8] The evident analogies showed by this pharmacophoric model with that developed by Clark et al. for quinuclidine derivatives related to **5**[9] suggested a common binding domain for both arylpiperazine and quinuclidine derivatives. However, the quinuclidine derivatives described by Clark can be considered, from the structural point of view, classical 5-HT_3 receptor antagonists (since they contain the generally recognized pharmacophore, i.e., basic nitrogen, carbonyl group, and aromatic ring), while our arylpiperazine ligands are somewhat atypical since a heterocyclic nitrogen atom replaces the carbonyl group and the interrelation between these two different classes in the interaction with the receptor is far from obvious.[10] These observations are at the basis of the design of a novel class of conformationally constrained 5-HT_3 receptor ligands **6**–**9**. In this paper, we report the synthesis, the pharmacological evaluation, and the results of extensive qualitative and quantitative structure–affinity relationship (SAFIR) studies (carried out by means of theoretical descriptors[11]—indirect approach) aimed at capturing information relevant to ligand–receptor interaction. Furthermore, a comparison between the results derived by the indirect approach and those obtained from the direct approach (which considers the energy minimized 3-D structures of the ligand–receptor complexes) was carried out in order to get further mechanistic insights into the binding mode multiplicity of the ligand gated ion channel 5-HT_3 receptors and to derive methodological considerations on the caveats of the two approaches.

Chemistry

Most of the target compounds (**6**–**9**) containing the *endo*-tropan-3-yl (*endo*-8-methyl-8-azabicyclo[3.2.1]oct-3-yl) moiety were easily synthesized by reaction of an excess of *endo*-8-methyl-8-azabicyclo[3.2.1]oct-3-ylamine[12] with the suitable γ-bromoester (**14**–**17**) available by bromination (NBS/dibenzoyl peroxide) of the appropriate *ortho*-methyl-substituted esters (**10**–**13**) (Scheme 1). Target tropane derivative **7a** was used as the starting material for the synthesis of nortropane derivative **7b** as shown in Scheme 2, while **7d** was the precursor of final derivatives **7c**, **7h** and **18** (Scheme 3).

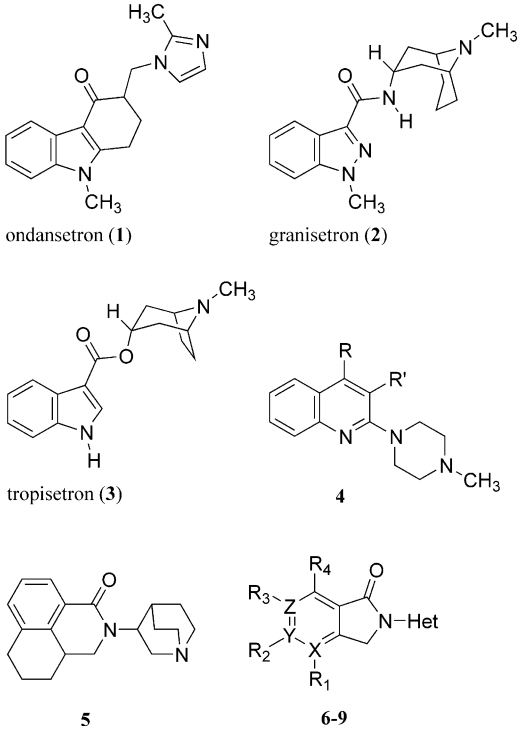

Chart 1.

Among the required starting esters **10**–**13**, naphthalene derivative **11a** was prepared according to the literature,[13] while its regioisomers **12a** and **13a** were synthesized by Stille cross-coupling[14] between triflates **23**[15] and **24** and tetramethylstannane as the key step (Scheme 4). Quinoline derivatives **11c**–**g** and **29** were synthesized from acid **25**[16] by means of standard methodologies, as shown in Scheme 5. While in the case of compound **26**, the alkylation with propyl iodide in the presence of sodium hydride led to a mixture of *O*-alkylated derivative **11g** with *N*-alkylated derivative **28**, a different result was obtained when 4(1H)-quinolinone **31**[17] was subjected to the same alkylation conditions (Scheme 6). Quite surprisingly, *O*-alkylated derivative **12e** only could be isolated, and the synthesis of the corresponding *N*-alkylated derivative **33** was achieved through the different approach shown in Scheme 7. Finally, the remaining starting quinoline derivatives **13b**–**f** were prepared from 2-aminoacetophenone (**36**) by the reaction sequence shown in Scheme 8.

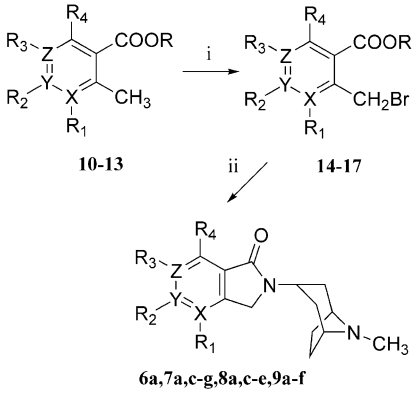

Scheme 1. Reagents: (i) NBS, dibenzoyl peroxide, CCl_4; (ii) *endo*-8-methyl-8-azabicyclo[3.2.1]oct-3-ylamine, EtOH.

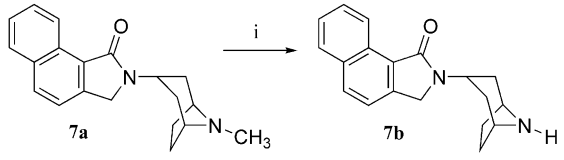

Scheme 2. Reagents: (i) α-chloroethyl chloroformate (ACE-Cl).

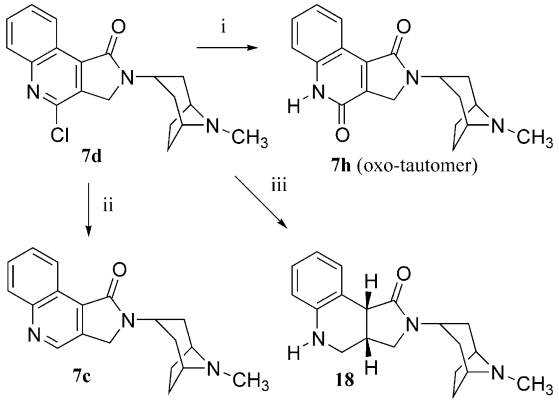

Scheme 3. Reagents: (i) HCl; (ii) H_2 (14 psi), Pd/C, Et_3N, EtOH; (iii) H_2 (50 psi), Pd/C, Et_3N, EtOH.

As far as the synthesis of the target quinuclidine derivatives was concerned, attempts were made to apply the simple chemistry described above for the preparation of tropane derivatives, and the condensation between 3-aminoquinuclidine and γ-chloroester **16b**[18] was studied as a model reaction.

Thus, commercial 3-aminoquinuclidine dihydrochloride (**38**) was converted into the free base with Na_2CO_3 in refluxing ethanol and was reacted with γ-chloroester **16b** to give, instead of the expected quinuclidine γ-lactam **8h**, a water soluble compound to which the structure of

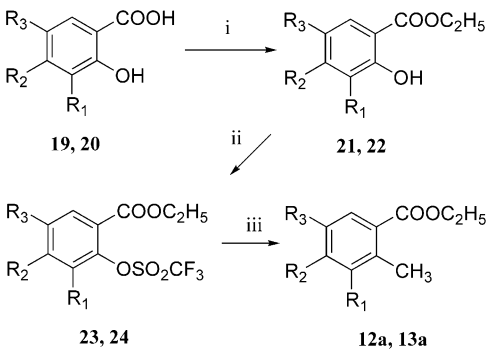

19, **21**, **23**, and **12a**, R_1 = H, R_2-R_3 = C_4H_4
20, **22**, **24**, and **13a**, R_3 = H, R_1-R_2 = C_4H_4

Scheme 4. Reagents: (i) (a) $SOCl_2$; (b) EtOH, Et_3N; (ii) $(CF_3SO_2)_2O$, C_5H_5N; (ii) $(CH_3)_4Sn$, LiCl, $Pd(PPh_3)_2Cl_2$, DMF.

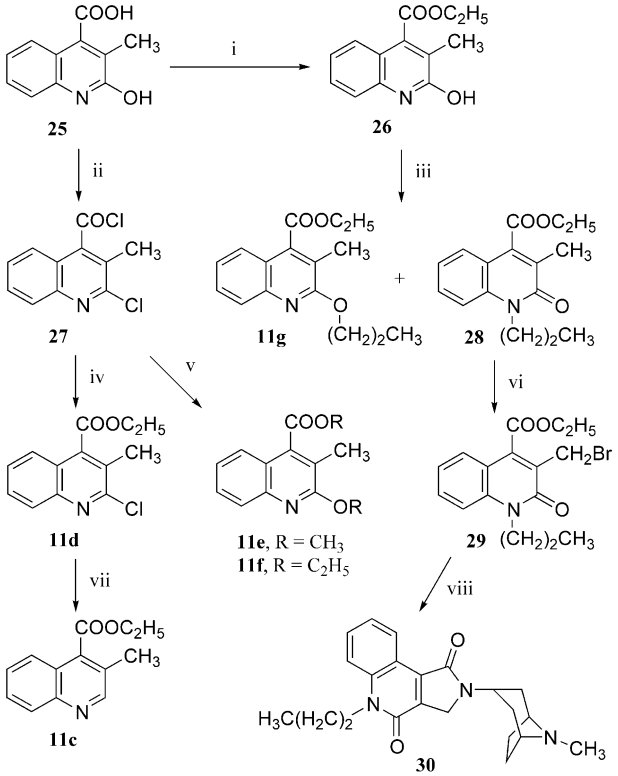

Scheme 5. Reagents: (i) (a) $SOCl_2$; (b) EtOH, Et_3N; (ii) $POCl_3$; (iii) (a) NaH, DMF; (b) $CH_3(CH_2)_2I$; (iv) EtOH, Et_3N; (v) NaH, ROH; (vi)NBS, dibenzoyl peroxide, CCl_4; (vii) H_2 (14 psi), Pd/C, Et_3N, EtOH; (vii) *endo*-8-methyl-8-azabicyclo[3.2.1]oct-3-ylamine, EtOH.

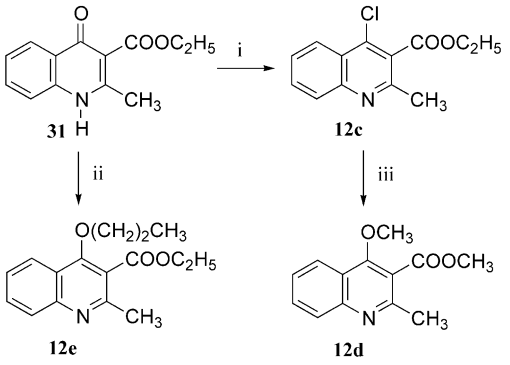

Scheme 6. Reagents: (i) $POCl_3$; (ii) (a) NaH, DMF; (b) $CH_3(CH_2)_2I$; (iii) NaH, MeOH.

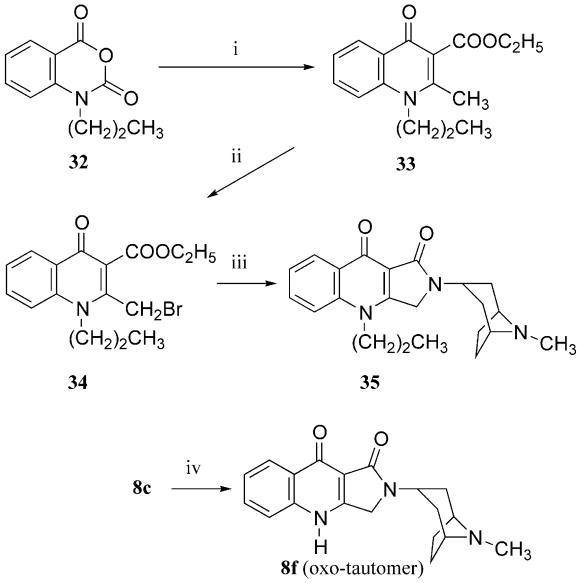

Scheme 7. Reagents: (i) CH_3–CO–CH_2–$COOC_2H_5$, NaH, DMA; (ii) NBS, dibenzoyl peroxide, CCl_4; (iii) *endo*-8-methyl-8-azabicyclo[3.2.1]oct-3-ylamine, EtOH; (iv) HCl.

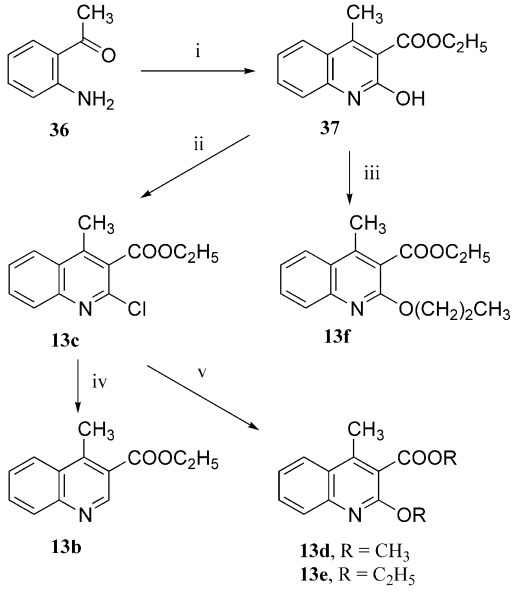

Scheme 8. Reagents: (i) (a) $ClCOCH_2COOC_2H_5$,CH_2Cl_2; (b) NaH, EtOH; (ii) $POCl_3$; (iii) (a) NaH, DMF, (b) $CH_3(CH_2)_2I$; (iv) H_2 (14 psi), Pd/C, Et_3N, EtOH; (v) NaH, ROH.

the inner salt **39** was tentatively assigned on the basis of its physicochemical and spectroscopic characteristics (Scheme 9). It appeared that between the two basic nitrogen atoms of 3-aminoquinuclidine the tertiary one was more reactive toward the chloromethyl moiety of **16b** and the reaction could not evolve toward the expected quinuclidine γ-lactam **8h**.

On the basis of these results, a new synthetic methodology was developed involving the protection of the more reactive tertiary nitrogen of 3-aminoquinuclidine with allyl bromide, the reaction with the suitable γ-haloester, and the deprotection with dipropylamine in the presence of $Pd(PPh_3)_2Cl_2$ (Scheme 10).[19]

It is noteworthy that this procedure could be conveniently applied without the isolation of quaternary ammonium salt intermediates **40** and **41**–**44**.[20] Moreover, the palladium catalyst played a key role in the deprotection since in its absence it could not be obtained. Finally, the procedure developed could be

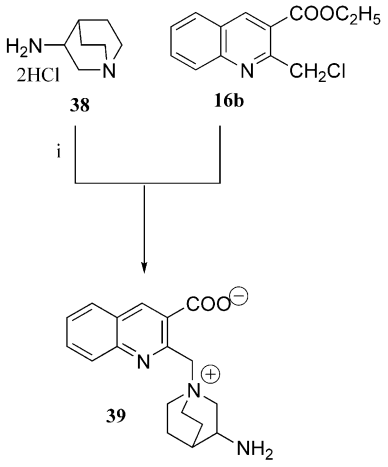

Scheme 9. Reagents: (i) Na_2CO_3, EtOH.

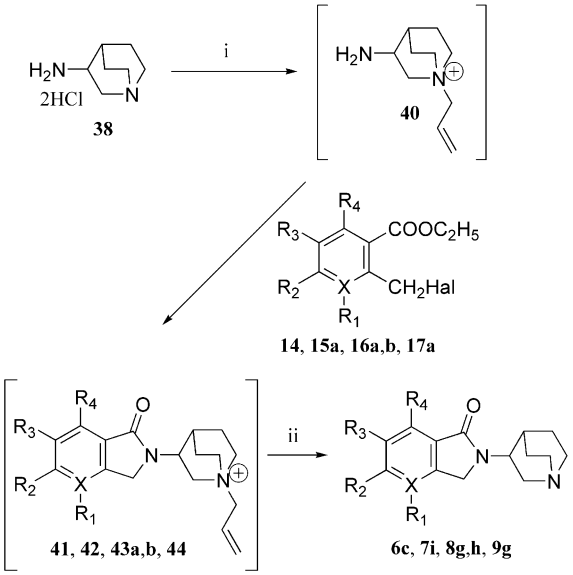

Scheme 10. Reagents: (i) (a) Na_2CO_3, EtOH, (b) CH_2=$CHCH_2Br$; (ii) $(CH_3CH_2CH_2)_2NH$, $Pd(PPh_3)_2Cl_2$, DMF.

conveniently used for the synthesis of the enantiomers of compounds **7i**, **8g**,**h**, and **9g**. When such compounds prepared from an enantiomer of 3-aminoquinuclidine were studied by ^{1}H NMR in the presence of a chiral complexing agent such as 1,1′-binaphthyl-2,2′-diylphosphoric acid (BNPPA),[21] the presence of a single enantiomer was detected.

Computational Procedures

Geometry optimization

The protonated structures of all the compounds studied were fully optimized by means of molecular orbital calculation, using the MOPAC 6.0 (QCPE 455) program. The three dimensional structure of ligands **7a**, **9a**, and **18**, solved by X-ray crystallography in our laboratory, were taken as the input for the AM1 optimization.[22] The starting geometry of the other derivatives considered were constructed by means of the Cerius2 program.[23]

Indirect approach

Ad-hoc modeling. The ad-hoc modeling consisted in comparing the van der Waals volume of the minimized structure of each ligand with the van der Waals volume of a supermolecule chosen as a template.[24] An automatic procedure to facilitate this goal has recently been published.[25]

In this work, two supermolecules have been considered: the first, sup-1, is aimed at rationalizing the binding features of compounds which are proved or assumed to be antagonists; the second, sup-2, is aimed at the rationalization of the binding affinity of all the ligands under study.

Two criteria have to be simultaneously satisfied by a ligand in order to be part of the tentative reference supermolecule, that is high affinity for the receptor and representativeness of unique structural features. Therefore, ligands **7g** and (*S*)-**7i** were chosen to constitute sup-1 and ligand (*R*)-**8h** was added to obtain sup-2. The ligands were superimposed, by a rigid fit procedure, minimizing the rms deviations with respect to three dummy atom pairs: (a) a dummy atom positioned on the NH^+ vector at 3.0 Å from the protonated nitrogen of the quinuclidine and tropane moiety; (b) a dummy atom positioned 3 Å from the carbonyl carbon, on the vector defined by the C=O bond (e.g., the midpoint between the oxygen lone pairs); (c) two dummy atoms positioned, respectively, 1.8 Å above and below the center of the aromatic plane of the phenyl ring located farthest from the protonated nitrogen. The dummy atoms represent an average position of receptor elements for potential binding interactions and tolerance in their rms deviations have to be allowed according to the nature of the interaction they represent (e.g., ionic > hydrogen bonding > dispersive) and the flexibility of the receptor side chains. All the other compounds were satisfactorily superimposed on the supermolecule by means of the same matching procedure, each ligand being superimposed on the analogous compound present in the supermolecule, or on its structurally closest compound.

The QUANTA98[26] molecular modeling software was used for molecular comparison and computation of van der Waals volumes. We considered the ad hoc-defined size and shape descriptors: V_{in} and V_{out} which are, respectively, the inner (intersection) and the outer van der Waals volume of the ligand considered with respect to the volume of the supermolecule (V_{sup}) and V_{dif} which is computed according to the formula $V_{dif} = (V_{in} - V_{out})/V_{sup}$.

Molecular descriptors and statistical treatment of data. The MOPAC output files were loaded into the CODESSA program[27] along with the experimental binding affinity data and a large number of global and fragment descriptors (topological, electrostatic, geometrical and quantum-chemical) were generated for each compound. The ad-hoc defined molecular size and shape descriptors, described above, were added as external descriptors.[11]

The search for the best correlation equation was achieved by means of the heuristic method, which accomplished a preselection of descriptors on the basis of their statistical significance.[27,28] Default values for control parameters and criteria were used: minimum squared correlation coefficient for one-parameter correlation to be considered significant, $R_{min} = 0.1$; *t*-test value for the descriptor to be considered significant in one-parameter correlation, $t_1 = 1.5$, *t*-test value for the descriptor to be considered significant in multi-parameter correlation, $t_2 = 3.0$; highest pair correlation coefficient of two descriptors scales, $r_{full} = 0.99$; significant intercorrelation level, $r_{sig} = 0.80$. Evaluation of the best correlation models was carried out by validation of the stability of each regression model by cross-validation techniques (i.e., the sensitivity of the model to the elimination of any single datum). The QSAR models reported in this paper were selected on the basis of the best statistical parameters and the largest diversity in the physical information content of the descriptors involved.

Direct approach

Docking, refinement and analysis of the complexes. Selected ligands were manually docked in the minimized average structure of the receptor previously obtained,[6] using the main criterium being the maximum complementarity between the position and characteristics of mutated residues putatively involved in ligand interaction and the pharmacophoric elements derived by the indirect approach.

In order to obtain an optimal complementarity of each ligand and the receptor cavity, several orientations were tested and the complexes were energy minimized by means of the CHARMM program.[29] The minimization

procedure consisted of 50 steps of steepest descent, followed by a conjugate gradient minimization until the rms gradient of the potential energy was less than 0.001 kcal/mol Å. The united atom force-field parameters, a 12 Å nonbonded cutoff and a dielectric constant $\varepsilon = 4r$ were used.

The choice of the 'best complex' among those obtained was performed on the basis of the following criteria: (a) the most favorable energetic state of the complex achieved by favorable energetic states of the individual components (CHARMM[29] energy) and (b) consistency in the binding preferences among the ligand considered.

Results

Qualitative structure–affinity relationships

The newly synthesized compounds were tested for their potential ability to displace [^{3}H]granisetron specifically bound to 5-HT$_3$ receptor in rat cortical membranes, in comparison with reference compounds 5-HT and granisetron, following a well-established protocol.[30] The results of the binding studies are summarized in Table 1.

SAFIR in the subclass of tropane derivatives. The binding studies performed on the compounds belonging to this subclass of 5-HT$_3$ receptor ligands revealed a relatively high affinity for the simplest representative **6a**; a 29-fold decrease in affinity resulted from the change of the favorable *endo*-stereochemistry into the *exo*-one, as in the case of **6b**.[17]

The introduction of an additional benzene ring on the different faces of the homocyclic portion of the byciclic system of compound **6a** (benzo-fusion) enhances the 5-HT$_3$ receptor affinity to a variable extent depending on the position occupied by the additional ring. Indeed, compound **7a**, possessing the additional benzo ring angularly fused in position *syn* with respect to the carbonyl moiety (*syn*-position), is about 2 orders of magnitude more potent than **6a**, while compound **8a**, with the linearly fused benzene ring (linear position), is only 2-fold more potent than **6a**. Finally, compound **9a**, showing the additional benzo ring in *anti*-position, is about 20-fold more potent than **6a**. *N*-Demethylation of the tropane moiety of compound **7a** does not produce significant effects on the 5-HT$_3$ receptor affinity. Similarly, both the transformation of the benz[*e*]isoindol-1-one nucleus of **7a** into the pyrrolo[3,4-*c*]quinolin-1-one heterocyclic system of **7c** (as a consequence of the introduction of a heterocyclic nitrogen atom) and the introduction of different substituents in 4-position of the latter tricyclic system (**7d**–**h**) produce only slight changes in the 5-HT$_3$ receptor affinity. The subnanomolar affinity shown by propyloxy derivative **7g** (the most potent representative of this subset of tropane derivatives) suggests that lipophilic substituents are easily accommodated into the receptor area interacting with 4-position of the tricyclic system.

Conversely, the partial saturation of the tricyclic system of **7c** leading to compound **18** has a detrimental effect on the 5-HT$_3$ receptor affinity probably because of the effect of deplanarization of tricyclic system on the electronic characteristics of the carbonyl moiety.

As has been observed in the case of compound **7a**, the introduction of a heterocyclic nitrogen atom in linearly fused **8a** has a negligible effect on the 5-HT$_3$ receptor affinity (c.f., **8a** with **8b**), while the subsequent introduction of different substituents in 9-position of the pyrrolo[3,4-*b*]quinoline system of compound **8b** (leading to compounds **8c**–**f**) produced complex SAFIR. In fact, unsubstituted derivative **8b** and chloro derivative **8c** showed the same potency (K_i values of 86 and 90 nM, respectively), while hydroxy derivative **8f** and methoxy derivative **8d** were more than 2-fold less potent ($K_i >$ 160 nM) and propyloxy derivative **8e** ($K_i = 23$ nM) was more than 7-fold more potent than **8d**. The most potent compound in this subset of ligands is propyloxy derivative **8e** which is nearly equipotent with its regioisomer **35** (Scheme 7), suggesting either some aspecific role of the *n*-propyl sidechain in the interaction with the 5-HT$_3$ receptor or the existence of multiple compensatory effects. Similar structural modifications in *anti*-fused **9a** produce an even more complex SAFIR trend. In fact, the transformation of the benz[*e*]isoindol-3-one nucleus of **9a** into the pyrrolo[3,4-*c*]quinolin-3-one heterocyclic system of **9b** is detrimental and only small substituents (Cl, OCH_3) are tolerated in the 4-position of the tricyclic system.

SAFIR in the subclass of quinuclidine derivatives. In analogy with the results obtained with the subclass of the tropane derivatives, the simplest representative of quinuclidine derivatives **6c** shows a relatively high 5-HT$_3$ receptor affinity and the benzo-fusion on the different faces of the homocyclic portion of the bicyclic system of compound **6c** produces significant increase in 5-HT$_3$ receptor affinity.

However, while both the *syn* (**7i**) and the *anti* (**9g**) benzo-fusion appear to have the same enhancing effects (about 2 and 1 order of magnitude, respectively) as those observed in the corresponding tropane derivatives (**7a** and **9a**), the linear one produces a 21-fold enhancement (1 order of magnitude higher than that observed in the linearly fused tropane derivative **8a**). All together, these results suggest a better adaptability of the quinuclidine derivatives in the interaction with the receptor. Interestingly, the transformation of the benz[*f*]isoindol-1-one nucleus of **8g** into the pyrrolo[3,4-*b*]quinolin-1-one heterocyclic system of **8h** (as a consequence of the introduction of a hydrogen bonding acceptor heterocyclic nitrogen atom) increases the 5-HT$_3$ receptor affinity by a factor of 5. This enhancing effect does not occur in the subclass of tropane derivatives.

The binding stereoselectivity of the most active quinuclidine derivatives **7i**, **8g**,**h**, and **9g** appears to be modulated by both the steric features of the tricyclic system and the presence of the hydrogen bonding acceptor heterocyclic nitrogen atom. The highest binding stereoselectivity

[(*R*)-enantiomer about two orders of magnitude more potent than (*S*)-enantiomer] is achieved by compound **8h** which shows a linear heterocyclic moiety and the presence of the hydrogen bonding acceptor. The removal of the hydrogen bonding acceptor reduces the binding stereoselectivity by one order of magnitude (c.f., **8h** with **8g**). The *syn* benzo-fused derivative **7i** shows both a reduction and an inversion of the stereoselectivity with respect to linearly fused derivatives **8h** and **8g**, while the binding of *anti*-fused derivative **9g** appears to be devoid of any stereoselectivity.

Indirect approach

Quantitative structure–affinity relationship analysis. The values of global and local molecular descriptors involved in the correlation which best model the variation in the binding affinity of these ligands are listed in Table 2, together with the cologarithmic form of the experimental affinity values.

The best linear correlation obtained involve the ad hoc derived size and shape descriptors, V_{dif} and V_{in}/V_{mol}:

Table 1. Binding affinities for the central 5-HT_3 receptor and effects on [^{14}C]guanidinium accumulation in NG 108-15 cells of compounds **6–9**, **18**, **30** and **35**

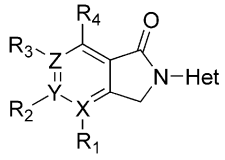

6-9

Compd	Het	X	Y	Z	R_1	R_2	R_3	R_4	K_i (nM) ±SEM[a]	Intrinsic efficacy[b]	EC_{50} (nM)	IC_{50} (nM)
6a	*endo*-Tropan-3-yl[c]	C	C	C	H	H	H	H	100±14			
6b	*exo*-Tropan-3-yl	C	C	C	H	H	H	H	2900±280			
6c	(*RS*)-Quinuclidin-3-yl[d]	C	C	C	H	H	H	H	160±19			
7a	*endo*-Tropan-3-yl	C	C	C	H	H	$-C_4H_4-$		1.2±0.23	Ant		12
7b	*endo*-Nortropan-3-yl[e]	C	C	C	H	H	$-C_4H_4-$		1.3±0.47			
7c	*endo*-Tropan-3-yl	C	N	C	H		$-C_4H_4-$		1.0±0.17			
7d	*endo*-Tropan-3-yl	C	N	C	Cl		$-C_4H_4-$		2.3±0.10			
7e	*endo*-Tropan-3-yl	C	N	C	OCH_3		$-C_4H_4-$		1.6±0.09			
7f	*endo*-Tropan-3-yl	C	N	C	OC_2H_5		$-C_4H_4-$		3.9±0.81			
7g	*endo*-Tropan-3-yl	C	N	C	O*n*-C_3H_7		$-C_4H_4-$		0.74±0.17			
7h	*endo*-Tropan-3-yl	C	N	C	OH		$-C_4H_4-$		1.1±0.36			
18									> 530			
30									8.1±2.7			
7i	(*RS*)-Quinuclidin-3-yl	C	C	C	H	H	$-C_4H_4-$		0.78±0.14			
(***S***)-**7i**	(*S*)-Quinuclidin-3-yl	C	C	C	H	H	$-C_4H_4-$		0.34±0.09	Ant		1.0
(***R***)-**7i**	(*R*)-Quinuclidin-3-yl	C	C	C	H	H	$-C_4H_4-$		1.8±0.49	PA	0.60	10
8a	*endo*-Tropan-3-yl	C	C	C	H	$-C_4H_4-$		H	52±23			
8b	*endo*-Tropan-3-yl	N	C	C		$-C_4H_4-$		H	86±37			
8c	*endo*-Tropan-3-yl	N	C	C		$-C_4H_4-$		Cl	90±19			
8d	*endo*-Tropan-3-yl	N	C	C		$-C_4H_4-$		OCH_3	> 160			
8e	*endo*-Tropan-3-yl	N	C	C		$-C_4H_4-$		O*n*-C_3H_7	23±0.30			
8f	*endo*-Tropan-3-yl	N	C	C		$-C_4H_4-$		OH	> 160			
35									34±12			
8g	(*RS*)-Quinuclidin-3-yl	C	C	C	H	$-C_4H_4-$		H	7.7±1.1			
(***S***)-**8g**	(*S*)-Quinuclidin-3-yl	C	C	C	H	$-C_4H_4-$		H	31±7.9	PA	3.0	25
(***R***)-**8g**	(*R*)-Quinuclidin-3-yl	C	C	C	H	$-C_4H_4-$		H	3.8±1.9	PA	0.50	50
8h	(*RS*)-Quinuclidin-3-yl	N	C	C		$-C_4H_4-$		H	1.6±0.16			
(***S***)-**8h**	(*S*)-Quinuclidin-3-yl	N	C	C		$-C_4H_4-$		H	87±17			
(***R***)-**8h**	(*R*)-Quinuclidin-3-yl	N	C	C		$-C_4H_4-$		H	0.83±0.30	PA	0.60	1.0
9a	*endo*-Tropan-3-yl	C	C	C	$-C_4H_4-$		H	H	4.9±0.50	Ant		5.0
9b	*endo*-Tropan-3-yl	C	C	N	$-C_4H_4-$			H	1000±280			
9c	*endo*-Tropan-3-yl	C	C	N	$-C_4H_4-$			Cl	280±160			
9d	*endo*-Tropan-3-yl	C	C	N	$-C_4H_4-$			OCH_3	410±210			
9e	*endo*-Tropan-3-yl	C	C	N	$-C_4H_4-$			OC_2H_5	> 160			
9f	*endo*-Tropan-3-yl	C	C	N	$-C_4H_4-$			O*n*-C_3H_7	> 1600			
(***S***)-**9g**	(*S*)-Quinuclidin-3-yl	C	C	C	$-C_4H_4-$		H	H	6.0±0.80	Ant		46
(***R***)-**9g**	(*R*)-Quinuclidin-3-yl	C	C	C	$-C_4H_4-$		H	H	6.6±1.5	A	0.13	
2									0.35±0.06			
5-HT									120±34			

[a]Each value is the mean ± SEM of three determinations and represents the concentration giving half the maximum inhibition of [^{3}H]granisetron specific binding to rat cortical membranes.
[b]A, pure agonist; PA, partial agonist; Ant, pure antagonist.
[c]Tropan-3-yl: 8-methyl-8-azabicyclo[3.2.1]oct-3-yl.
[d]Quinuclidin-3-yl: 1-azabicyclo[2.2.2]oct-3-yl.
[e]Nortropan-3-yl: 8-azabicyclo[3.2.1]oct-3-yl.

Table 2. 5-HT_3 binding affinities and theoretical descriptors of the protonated form of selected ligands from Table 1

Compd	pK_i	V_{dif} (sup-1)	V_{in} (sup-2) (Å^3)	V_{in}/V_{mol} (sup-2)	V_{out} (sup-2) (Å^3)	V_{dif} (sup-2)	P (N)	(O)-WCPSA (Å^2)	EHOMO (eV^{-1})	$f_{aa'}$-SAS (Å^2)	f_a-FNSA-2	f-CIC
6a	7.00	0.5095	223.25	0.9038	23.250	0.4806	0.9242	0.0158	−11.336	123.826	−0.0901	2.00
6c	6.80	0.3419	195.63	0.9174	17.620	0.4288	0.9045	0.0235	−12.194	142.876	−0.0901	2.00
7a	8.92	0.7208	280.88	0.9554	13.120	0.6450	0.9244	0.0198	−11.069	113.404	−0.0661	6.75
7b	8.89	0.6675	262.25	0.9541	12.63	0.6013	0.9075	0.0171	−10.867	111.027	−0.0655	6.75
7c	9.00	0.7225	278.00	0.9632	10.630	0.6441	0.9238	0.0169	−11.127	105.031	−0.0677	2.00
7d	8.64	0.7340	288.13	0.9455	16.620	0.6540	0.9236	0.0241	−12.038	142.906	−0.065	2.00
7e	8.80	0.7706	297.88	0.9559	13.75	0.6844	0.9242	0.0141	−10.984	86.477	−0.0597	2.00
7f	8.41	0.6556	284.50	0.8724	41.630	0.5850	0.9244	0.0150	−10.803	107.159	−0.0551	2.00
7g	9.13	0.8155	310.38	1.0000	0.000	0.7052	0.9244	0.0202	−11.315	143.033	−0.0559	2.00
7h	8.96	0.734	281.75	0.9649	10.25	0.6540	0.9234	0.0168	−11.322	98.697	−0.0695	2.00
30	8.09	0.6340	289.25	0.8510	50.630	0.5748	0.9240	0.0147	−10.963	71.815	−0.0613	4.00
(***S***)**-7i**	9.47	0.7075	254.00	1.0000	0.000	0.6119	0.9045	0.0171	−10.953	112.213	−0.0651	6.75
(***R***)**-7i**	8.75	—	243.00	0.9567	11.000	0.5589	0.9045	0.0171	−10.953	112.213	−0.0651	6.75
8a	7.28	0.5501	264.13	0.8969	30.370	0.5631	0.9245	0.0177	−10.833	111.402	−0.0829	6.00
8b	7.07	0.5407	257.63	0.8965	29.750	0.5489	0.9241	0.0154	−11.019	88.325	−0.0806	0.00
8c	7.05	0.5247	255.00	0.8858	32.880	0.5351	0.9240	0.0173	−11.213	114.168	−0.0678	0.00
8e	7.64	0.5000	271.25	0.8242	73.000	0.4776	0.9247	0.0083	−11.220	83.208	−0.0408	0.00
35	7.47	0.5442	283.88	0.8402	54.000	0.5538	0.9244	0.0162	−10.866	120.240	−0.0687	2.00
(***S***)**-8g**	7.51	—	242.38	0.9472	13.500	0.5513	0.9041	0.0204	−11.946	115.474	−0.0832	6.00
(***R***)**-8g**	8.42	—	251.75	0.9965	0.880	0.6043	0.9041	0.0204	−10.946	115.474	−0.0832	6.00
(***S***)**-8h**	7.06	0.7075	238.38	0.9469	13.370	0.5420	0.9053	0.0198	−11.436	118.758	−0.0817	2.00
(***R***)**-8h**	9.08	—	248.25	1.0000	0.000	0.5980	0.9053	0.0198	−11.436	118.758	−0.0817	2.00
9a	8.31	0.4899	256.75	0.8774	35.880	0.5321	0.9243	0.0210	−10.946	112.512	−0.0762	6.75
9b	6.00	0.3092	223.38	0.7879	60.120	0.3933	0.9239	0.0215	−11.407	137.343	−0.0809	0.00
9c	6.55	0.3656	240.00	0.7980	60.750	0.4318	0.9237	0.0164	−11.434	119.839	−0.0696	0.00
9d	6.39	0.3635	236.50	0.7956	60.750	0.4234	0.9243	0.0172	−11.101	107.075	−0.0617	0.00
(***S***)**-9g**	8.22	0.4613	233.75	0.9064	24.130	0.5050	0.9045	0.0209	−11.074	108.902	−0.0757	6.75
(***R***)**-9g**	8.18	—	233.75	0.9047	24.63	0.5037	0.9045	0.0209	−11.074	108.902	−0.0757	6.75

$$\begin{aligned} pK_i &= 4.367(\pm 0.399) + 6.165(\pm 0.681)V_{dif}(\text{sup}-1) \\ R^2 &= 0.796,\ \ n = 23,\ \ F = 82.03, \\ s^2 &= 0.2206,\ \ R^2_{cv} = 0.765 \end{aligned} \quad (1)$$

$$\begin{aligned} pK_i &= 2.382(\pm 0.705) + 11.003(\pm 1.253)V_{dif}(\text{sup}-2) \\ R^2 &= 0.711,\ \ n = 28,\ \ F = 64.03, \\ s^2 &= 0.2801,\ \ R^2_{cv} = 0.7052 \end{aligned} \quad (2)$$

$$\begin{aligned} pK_i &= -2.573(\pm 1.763) + 11.554(\pm 1.927) \\ &\quad \times V_{in}/V_{mol}(\text{sup}-2) \\ R^2 &= 0.580,\ \ n = 28,\ \ F = 35.92, \\ s^2 &= 0.4072,\ \ R^2_{cv} = 0.5847 \end{aligned} \quad (3)$$

where R is the correlation coefficient, n is the number of compounds, F is the value of the Fisher ratio, s is the standard deviation, and R_{cv} is the cross-validated correlation coefficient; the numbers in parentheses are the 95% confidence intervals of the regression coefficient and of the intercept.

The theoretical descriptor involved in eq (1) is designed to explain the variation in the binding affinities of the antagonists considered in this study, while the Supermolecule-2 possesses all the necessary information to rationalize the binding modes of the ligands considered without taking account their functional activities [eqs (2)–(11)].

The linear models [eqs (1)–(3)] suggest that optimization of the binding affinity is achieved by maximizing the amount of bulk in one ligand in the van der Waals volume region delimited by V_{sup}. Intermolecular structural complementarity is then quantified by the extent and the balance of dispersion forces and steric interactions.

A significant improvement in the linear regressions is obtained by using theoretical molecular descriptors which represent the propensity of the ligands to give additional intermolecular interactions.[31] To this regard, only the enantiomers characterized by the highest binding affinity are considered in the following QSAR analysis since the molecular orbital descriptors derived for the isolated molecules cannot take into account the chirality requirements of the receptor binding site.

For comparison purposes, eqs (4) and (5) show the performance of the ad hoc molecular descriptors on the subset of 24 ligands:

$$\begin{aligned} pK_i &= 2.285(\pm 0.671) + 10.177(\pm 1.186)V_{dif}(\text{sup}-2) \\ R^2 &= 0.770,\ \ n = 24,\ \ F = 73.62, \\ s^2 &= 0.246,\ \ R^2_{cv} = 0.7052 \end{aligned} \quad (4)$$

$$\begin{aligned} pK_i &= -3.140(\pm 1.677) + 12.25(\pm 1.843) \\ &\quad \times V_{in}/V_{mol}(\text{sup}-2) \\ R^2 &= 0.668,\ \ n = 24,\ \ F = 44.19, \\ s^2 &= 0.3556,\ \ R^2_{cv} = 0.5847 \end{aligned} \quad (5)$$

In the models obtained, specific and non-specific polar interactions are codified by surface area descriptors or charged contact surface area descriptors[31] computed on ligand fragments:

$$\begin{aligned} pK_i &= -1.249(\pm 0.123) + 12.98 \\ &\quad \times (\pm 1.297) V_{in}/V_{mol}(sup-2) - 36.439 \\ &\quad \times (\pm 7.441) f_a - FNSA \\ R^2 &= 0.845, \quad n = 24, \quad F = 57.17, \\ s^2 &= 0.1739, \quad R^2_{cv} = 0.802 \end{aligned} \tag{6}$$

$$\begin{aligned} pK_i &= -0.684(\pm 0.102) + 10.891 \\ &\quad \times (\pm 1.363) V_{in}/V_{mol}(sup-2) - 0.023 \\ &\quad \times (\pm 0.005) f_{aa'} - SAS \\ R^2 &= 0.835, \quad n = 24, \quad F = 52.99, \\ s^2 &= 0.1853, \quad R^2_{cv} = 0.778 \end{aligned} \tag{7}$$

The involvement of the solvent accessible surface area of the fractional negative partial surface area (f_a-FNSA) of the pyrrolidone moiety and of the heterocyclic nucleus ($f_{aa'}$-SAS) leads to a significant improvement in the statistics and predictivity of eq (5).

These indices may be assumed to rationalize the electrostatic component of the binding adjustments modulating the binding affinity once the main docking has been accomplished and helps to overcome the main drawback of the V_{in}/V_{mol} descriptor which considers equally active, irrespective of their size, all the ligands whose V_{in} coincides with V_{mol}.

Moreover, the contribution of two key structural elements for receptor binding is taken into account in the following equations:

$$\begin{aligned} pK_i &= -1.804(\pm 0.133) + 13.006 \\ &\quad \times (\pm 1.437) V_{in}/V_{mol}(sup-2) - 123.51 \\ &\quad \times (\pm 28.51)(O)\text{-}WCPSA \\ R^2 &= 0.811, \quad n = 24, \quad F = 44.93, \\ s^2 &= 0.2123, \quad R^2_{cv} = 0.759 \end{aligned} \tag{8}$$

$$\begin{aligned} pK_i &= 35.12(\pm 9.07) + 10.239(\pm 0.952) V_{dif}(sup-2) \\ &\quad - 35.754(\pm 10.61) P(N) \\ R^2 &= 0.858, \quad n = 24, \quad F = 63.70, \\ s^2 &= 0.1586, \quad R^2_{cv} = 0.822 \end{aligned} \tag{9}$$

(O)-WCPSA is the weighed charged partial surface area of the carbonyl oxygen, and, being reflected by the negative value of the regression coefficient, it indicates the importance of hydrogen bonding capability of this moiety.

The addition of the valency-related bond order descriptor for the nitrogen atom [P(N)] as a second parameter in eq. (9) adjusts the model in order to describe the different reactivity characteristics of the quinuclidine and tropane protonated nitrogen atoms toward the establishment of hydrogen bond interactions with the receptor.

Improvement of eq (5) can also be achieved by considering the energy of the highest occupied molecular orbital (E_{HOMO}), which, being localized on the conjugate heteroaromatic moieties, describes the availability of the π-orbitals for receptor interactions.

$$\begin{aligned} pK_i &= 10.859(\pm 3.227) + 11.670 \\ &\quad \times (\pm 1.327) V_{in}/V_{mol}(sup-2) + 1.204 \\ &\quad \times (\pm 0.258) E_{HOMO} \\ R^2 &= 0.837, \quad n = 24, \quad F = 53.95, \\ s^2 &= 0.1826, \quad R^2_{cv} = 0.802 \end{aligned} \tag{10}$$

Finally, the predictivity of eq (7) is improved by considering the complementary information content of the quinuclidine and tropane moieties (f-CIC)[32] that explains the portion of the biological response elicited by non-specific interactions (dispersion forces).

$$\begin{aligned} pK_i &= 0.232(\pm 0.012) + 11.211 \\ &\quad \times (\pm 1.206) V_{in}/V_{mol}(sup-2) + 38.957 \\ &\quad \times (\pm 6.220) f_a - FNSA - 2 + 0.098 \\ &\quad \times (\pm 0.032) f - CIC \\ R^2 &= 0.898, \quad n = 24, \quad F = 58.90, \\ s^2 &= 0.1196, \quad R^2_{cv} = 0.851 \end{aligned} \tag{11}$$

The comparison between the experimental binding affinities and those calculated by eq (11) is shown in Fig. 1. On the basis of its statistical indices and predictive power, the latter equation can be considered the best QSAR equation to describe the variation in the 5-HT_3 receptor binding affinity within the set of the ligands considered.

Direct approach

3-D models of the ligand–receptor complexes. Selected ligands were docked in the putative binding site in order to test, on a quantitative ground, the hypothesis that, though sharing the same binding site, different binding modalities might exist for agonists and antagonists.[6] The binding site was individuated and proposed on the basis of previously derived pharmacophoric hypotheses, and of an extensive analysis of the experimental results on point mutation effects obtained for all the members of the receptor family. Table 3 lists the energy contribution of the most important binding site residues to the total interaction energy of the ligands considered. Moreover, the degree of conservation of these residues among different species (human, ferret, guinea pig, rat

and mouse) and among the members of the Cys loop family of LGIC receptor family (nACh, $GABA_A$, Gly, and 5-HT_3 receptors) is also reported in Table 3. The binding paradigm, derived on the basis of pharmacophoric hypotheses previously reported and supported by the SAFIR and QSAR analysis described in this study, is fully satisfied by considering the establishing of (a) a charge-assisted hydrogen bonding interaction between the positively charged head of the ligands and the negatively charged carboxylic tail of E171 (first receptor subunit), for the antagonists, or of E84 (second receptor subunit) for the agonists; (b) a hydrogen bonding interaction between the ligand nitrogen or oxygen acceptor atom and Y169 (first receptor subunit) for the antagonists, or H80 (second receptor subunit) for the agonists; (c) specific (π–π) interactions between the ligand aromatic moiety and F104 and/or F158; and finally (d) short-range dispersion interactions between ligand substituents and I55, L99 and/or L119. These key interactions are enhanced by several other aminoacid interactions, which are listed in the table.

A decomposition of the interaction energy of the ligands into the van der Waals, electrostatic and hydrogen bonding contributors revealed that, in the model presented here, the agonists and antagonists achieved a good (~ -3.8 kcal/mol) hydrogen bonding interaction with E84 and E171, respectively. However, all the ligands considered are able to establish electrostatic and van der Waals interactions with both the acidic residues. It is interesting to note that both these acidic residues are strictly conserved among the 5-HT_3 receptors of different species, while they are not conserved among other members of the receptor family. They are, therefore, both good candidates for ligand recognition. Moreover, the residue corresponding to E171 (Y167 in nAChR α subunit) has been suggested to interact directly with ammonium in the nAChR,[33] while E84 is located in a β-strand constituted by aminoacids that have been shown to regulate the receptor conformational equilibrium, together with P90, the cardinal residue for receptor function.[34]

Functional activity

The measurement of [^{14}C]guanidinium uptake in the presence of substance P (SP) appears to be a rapid and reliable method to assess the functional properties of 5-HT_3 agents in NG108-15 hybridoma cells.[35] Owing to the similarities existing between 5-HT_3 receptors present in NG108-15 cells and those of rat cerebral cortex,[36] relevant inferences can be drawn from this pharmacological model about the functional properties of the ligands at central 5-HT_3 receptors. Accordingly, the potential 5-HT_3 agonist/antagonist activity of some selected compounds was assessed in vitro on the 5-HT_3 receptor-dependent [^{14}C]guanidinium uptake in NG 108-15 cells. The results of these functional studies are summarized in Table 1.

In the presence of substance P (10 μM) quinuclidine derivative (*R*)-**9g** increased in a concentration-dependent manner the uptake of [^{14}C]guanidinium into NG 108-15 cells with an EC_{50} value of about 0.13 nM, showing itself to act as a very potent 5-HT_3 agonist. The maximum uptake increase was similar to that of 5-HT and was antagonized by ondansetron (**1**). Moreover, this compound was unable to inhibit the effects of 5-HT (1 μM).

On the other hand, quinuclidine derivative (*S*)-**8g** appeared to act as a partial agonist with an EC_{50} value of 3.0 nM since it stimulated [^{14}C]guanidinium uptake up to a maximal level equal to about 2/3 of that reached with a saturating concentration of 5-HT (1 μM). Furthermore, in agreement with its partial agonist properties, (*S*)-**8g** reduced, in a concentration-dependent manner ($IC_{50} = 25$ nM), [^{14}C]guanidinium uptake due to 1 μM 5-HT plus 10 μM SP, down to the level reached in the presence of (*S*)-**8g** alone at a saturating concentration (0.1–1.0 μM). Similarly, the closely related compounds (*R*)-**7i**, (*R*)-**8g**, and (*R*)-**8h** behaved as partial agonists.

Finally, compounds **7a**, (*S*)-**7i**, **9a**, and (*S*)-**9g** showed clear-cut antagonist properties with IC_{50} values ranging from 1.0 to 46 nM.

It is noteworthy that both tropane derivatives tested in this functional assay (**7a** and **9a**) showed clear-cut antagonist properties, while the studied quinuclidine derivatives [the enantiomers of compounds **7i**, **8g**, and **9g**, and compound (*R*)-**8h**] showed the full range of 5-HT_3 receptor intrinsic efficacies (full agonist, partial agonist and antagonist). In particular, the behavior of these quinuclidine derivatives in the 5-HT_3 receptor-dependent [^{14}C]guanidinium uptake in NG 108-15 cells appeared to be affected by the chirality of the attachment of quinuclidine moiety to the tricyclic heteroaromatic system. In fact, the enantiomers of compounds **7i** and **9g** possessing *S* configuration showed antagonist properties, while the corresponding (*R*)-enantiomers were partial agonist and full agonist, respectively. However, the comparison of the intrinsic efficacies of compounds **7i**, **8g**, and **9g** suggests a possible role of the steric features of the heteroaromatic portion in determining the intrinsic efficacy of these quinuclidine derivatives.

In vivo activity. In addition to the 5-HT_3 receptor-dependent accumulation of [^{14}C]guanidinium uptake in NG 108-15 cells, the potential agonist/antagonist activity of two selected compounds, as representative of the two subclasses, was assessed on the 5-HT_3 receptor-dependent Bezold–Jarisch reflex in urethane-anesthetized rats. Indeed, none of these compounds mimicked the effects of 5-HT in this test (up to the dose of 120 μg/kg iv). In agreement with the data obtained on NG 108-15 cells, investigations on urethane-anesthetized rats confirmed the 5-HT_3 receptor antagonist properties of compounds **7a** and (*S*)-**7i**. Dose–response curves indicated that half-maximal blockade of the reflex bradycardia elicited by a bolus iv injection of 5-HT (30 μg/kg) was obtained with 2.8 μg/kg of **7a**, or 181 μg/kg of (*S*)-**7i** (iv) (means of three determinations) injected 5 min before indoleamine administration. Significant reduction of the 5-HT-evoked bradycardia was still observed

15 min after the iv injection of **7a** ($ID_{50} = 5.9$ μg/kg). Studies of the effects of classical 5-HT_3 receptor antagonists in the same test indicated that half maximal blockade of the reflex bradycardia due to 30 μg/kg iv of 5-HT was obtained with 0.45 μg/kg iv of zacopride, 3.0 μg/kg iv of tropisetron or 3.6 μg/kg iv of ondansetron (means of three determinations) injected 5 min before indoleamine administration.[37]

Furthermore in a preliminary study, compounds **7a**, (*S*)-**7i** and **9a** (at the doses of 0.01, 1.0, and 0.01 mg/kg ip, respectively) prevented scopolamine-induced amnesia in the mouse passive avoidance test[38] reaching entrance latency values comparable to those produced by saline-treated mice. At 10-fold lower doses, all compounds proved to be completely ineffective (Fig. 2). At active doses, **7a**, (*S*)-**7i** and **9a** did not enhance the entrance latency in unamnestic mice with respect to the control group (data not shown). No differences were observed in the various entrance latencies of every group in the training session of the passive avoidance test (Fig. 2). The behavior of animals treated with active doses of compounds **7a**, (*S*)-**7i** and **9a** was undistinguishable from that of controls, with no modification in motor coordination, spontaneous motility or inspection activity as revealed by rota-rod, Animex, and hole-board test, respectively (data not shown).

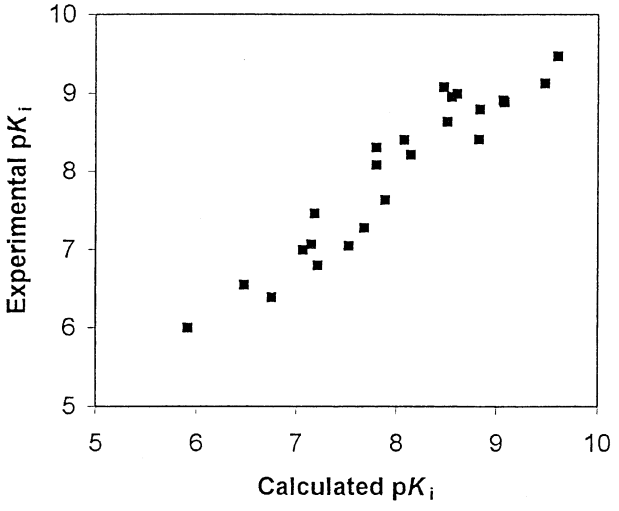

Figure 1. Calculated versus experimental 5-HT_3 binding affinities according to eq (11).

Discussion

The interactions at the central 5-HT_3 receptor

The work we performed on the arylpiperazine ligands led to the development of an initial three-component model for the interaction of quipazine derivatives with central 5-HT_3 receptor, which was updated as the work progressed.[8] Thus, the final model involves: (1) a charge-assisted hydrogen bond between a protonated nitrogen atom and a negatively charged carboxylic amino acid residue in the receptor, (2) a hydrogen bonding interaction between a ligand acceptor atom and a suitable H-bond donor in the receptor, (3) a specific interaction between an aromatic ring and a suitable amino acid residue in the receptor, and (4) a zone in which short range (e.g., van der Waals) interactions take place.

The interaction model proposed[8] shows evident analogies with that developed by Clark for quinuclidine derivatives related to **5**,[9] and therefore a common binding domain for both arylpiperazine and quinuclidine derivatives may be assumed.

Interestingly, most of the qualitative and quantitative SAFIR trends observed in the classes of 5-HT_3 receptor ligands considered in this work are consistent with the above-described model. In fact, the molecular

Table 3. Energy contributions of the most important binding site residues to the total interaction energy of selected ligands, and degree of conservation of the residues among different species (human, ferret, guinea pig, rat and mouse) and among the members of the cys loop family of LGIC receptor family (nACh, $GABA_A$, Gly, and 5-HT_3)

Residue	Specie specificity	Family specificity	**7g** (Kcal/mol)	**7i** (Kcal/mol)	**4a** (Kcal/mol)	**9g** (Kcal/mol)
First subunit (analogous to subunit α1, in the nAChR)						
E171	c[a]	nc[a]	−15.80	−10.93	−14.31	−5.74
Y169	c	c (nc in nACh)	−10.54	−9.91	−8.72	−3.24
F104	c	c	−3.79	−1.58	−3.12	−1.34
F158	c	nc	−3.12	−2.68	−4.91	−2.63
I55	c	Conservative mutation	−2.23	−2.32	−3.74	−2.39
L61	c	Conservative mutations	−3.52	−2.75	−2.50	−2.26
I62	c	Conservative mutations	−1.98	−2.37	−0.8	−1.62
L99	c	nc	−3.25	−2.13	−2.16	−1.10
S117	c	c	−7.33	−1.22	−0.85	−2.75
L119	c	nc	−2.50	−2.10	−1.33	−2.36
Second subunit (analogous to subunit γ, in the nAChR)						
W25	c	Conservative mutations	−2.04	−2.45	−1.81	−1.61
Q82	Conservative mutations	nc	−6.63	−5.51	−0.84	−2.83
H80	Conservative mutations	nc	−0.69	−2.06	−1.01	−3.26
E84	c	nc	−7.58	−5.08	−6.60	−13.66
V79	c	Conservative mutation	−5.69	−3.12	−4.45	−3.57

[a]c, conserved; nc, not conserved.

descriptors involved in the QSAR models obtained for these classes of ligands highlight the same pharmacophoric points. For example, the long-range interaction component is explicitly considered in eq (9) by the valency-related bond order descriptor P(N) which takes into account the attitude of the protonated nitrogen to act as a proton donor (quinuclidine > tropane) and/or form charge reinforced hydrogen-bonding interactions (pharmacophoric point 1). The modulation in the binding affinity data values, which is assumed to be due to a hydrogen-bonding interaction between the carbonyl oxygen atom and a suitable H-bond donor of the receptor (pharmacophoric point 2) is accounted for by the partial negative surface area of the heteroaryl moiety pyridine ring (f_a-FNSA) [eq (7)] and by the weighed charged partial surface area descriptor (O)-WCPSA [eq (8)] which rationalizes the electrostatic component of this H-bonding interaction. Moreover, potential π–π drug–receptor interactions (pharmacophoric point 3) are parameterized by the descriptors involved in eqs (5) and (9). In fact, $f_{aa'}$-SAS and E_{HOMO} describe the reactivity of the conjugate heteroaromatic moieties from a geometric and energetic point of view. However, most of the variation in the binding affinity of this set of ligands is captured by molecular descriptors which encode the potential for dispersion-type interactions [V_{dif}(sup-1, sup-2), V_{in}/V_{mol}(sup-2), and f-CIC] (pharmacophoric point 4), therefore strength and specificity might both arise from the cumulating and interplay of many weak forces between the ligand and its target receptor.

Thus, the results obtained by indirect approaches applied to several series of 5-HT_3 receptor ligands show that structurally different ligands share the same pharmacophoric characteristics,[39] and this usually leads to the assumption that a common binding domain might exist.

However, the results obtained by energy minimization of the complexes (direct approach) regarding selected structurally different 5-HT_3R ligands confirmed, on a quantitative ground, the hypothesis recently advanced[6] that, though sharing the same pharmacophoric features and the same binding site, different binding modalities might exist for agonists and antagonists. This is shown in Figure 3, where details of agonist (Fig. 3a) and antagonist (Fig. 3b) binding sites are reported. Agonist (*R*)-**9g** and antagonist (*S*)-**7i** have been used to emphasize that the main difference in the binding mode rests in the aminoacids which acts as counterion for the protonated nitrogen, and those implicated in the hydrogen bonding. However, alternative hypotheses might be suggested by the analysis of the 3-D models and have to be verified by a comparative molecular dynamics analysis of a wide series of ligands, with full range of intrinsic affinities. In particular, the mutual positions of the two negatively charged residues involved in electrostatic interactions with the agonists and the antagonists, and the topography of the interface crevice suggest that, in a dynamic view, the cationic head of the ligands might give rise to a sort of transiently concomitant resonant interaction with the two glutamate residues, with a preference for E84 for the agonists and for E171

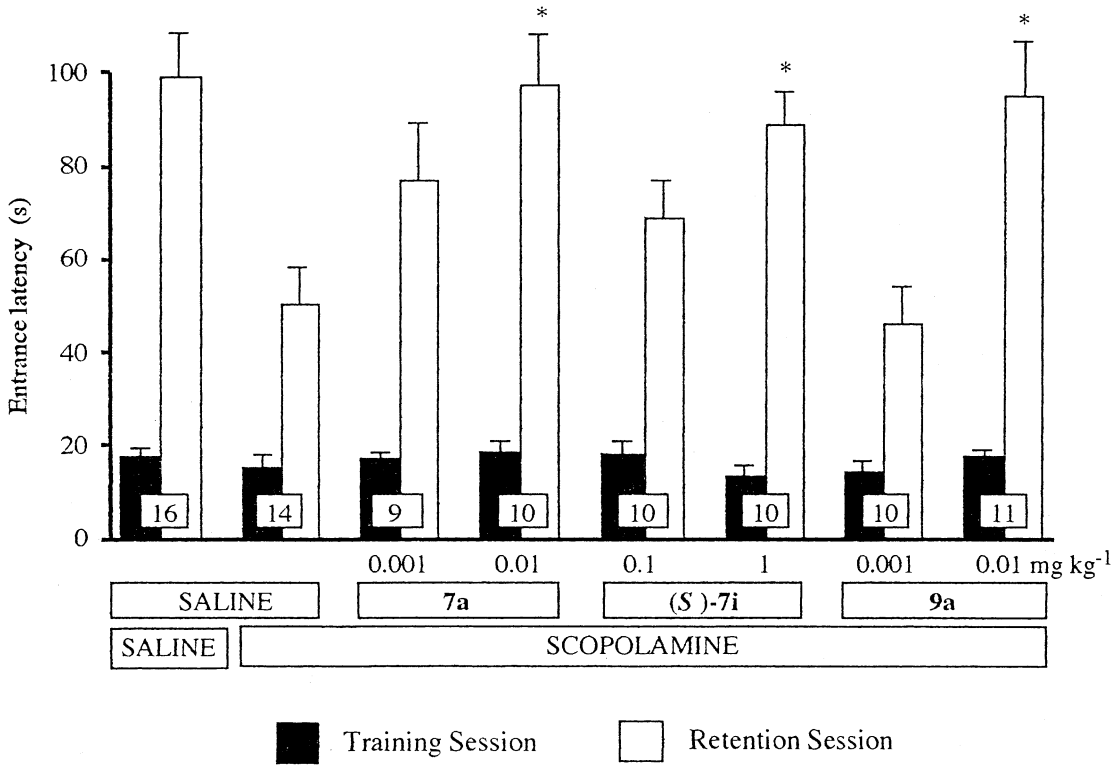

Figure 2. Effect of compounds **7a**, (*S*)-**7i** and **9a** on amnesia induced by scopolamine (1.5 mg/kg ip) in the mouse passive avoidance test. All the compounds were administered ip 20 min before the training session, while scopolamine was injected immediately after. Vertical lines give SE of the mean. The number of mice treated is reported inside the columns. * $p < 0.01$ in comparison with scopolamine-treated mice.

for the antagonists. Moreover, other molecular determinants might be responsible for the activation/inactivation of the receptor.

A comparison between the binding hypotheses derived by the indirect and the direct approaches for the antagonists is reported in Figure 3c and d, respectively. In fact, in Figure 3c, the arylpiperazine derivative **4a** has been superimposed to the supermolecule sup-1 composed of quinuclidine derivative (*S*)-**7i**, and tropane derivative **7g**. It is noteworthy that the alignment of the dummy atoms (which represent the average position of the receptor elements for potential binding interactions) is quite strict for those receptor features which may establish dispersive (short range) and/or hydrogen bonding (short/medium range) interactions, while a large tolerance is allowed for the interaction involving the protonated nitrogen. The importance of this structural feature, which was highlighted by several authors,[9,10b] implies that the presence of a basic nitrogen in the structure of the ligands is necessary in a preliminary step of receptor recognition (long-range interaction); then an ionic and/or charge reinforced hydrogen bonding interaction can be established during the docking process, depending on the nature of the ligand. Evidence from the affinity of quaternary salts reported in the literature[8a,10b] supports this hypothesis and further investigations are in progress in order to clarify the role of the $N–H^+$ moiety in the different classes of ligands. However, the superimposition of the same ligands docked in the 5-HT_3 binding site, as derived by the energy minimized complexes, reveals that the alignment criteria applied for the aromatic moieties in the indirect approach are much more severe than necessary; in fact, the binding site crevice is pretty tolerant in this region.

Moreover, the hypothesis that different binding modes could be operative for the 5-HT_3 receptor is substantiated by the differences observed in the binding stereoselectivity of quinuclidine derivatives **7i**, **8g**,**h**, and **9g**. The enantiomer of compound **7i** with *S* configuration is about one order of magnitude more potent than the (*R*) enantiomer in analogy with the results described for zacopride (**45**),[40] and can be very easily accommodated into the above-described model (Fig. 3). On the other hand, compound **8h** shows both an enhancement and an inversion in the stereoselectivity, the (*R*)-enantiomer being about two orders of magnitude more potent than the (*S*)-enantiomer in analogy with the results described for **46**.[40] Interestingly, compound **46**, which represents the 3-oxo derivative of **7i**, shows an 18-fold lower affinity and contains two potential H-bond acceptors in its structure as compared with compound **8h** (Chart 2).

The literature on this subject reveals that besides **46**, quinuclidine derivatives **47**,[40] and **48**[41] also possess both

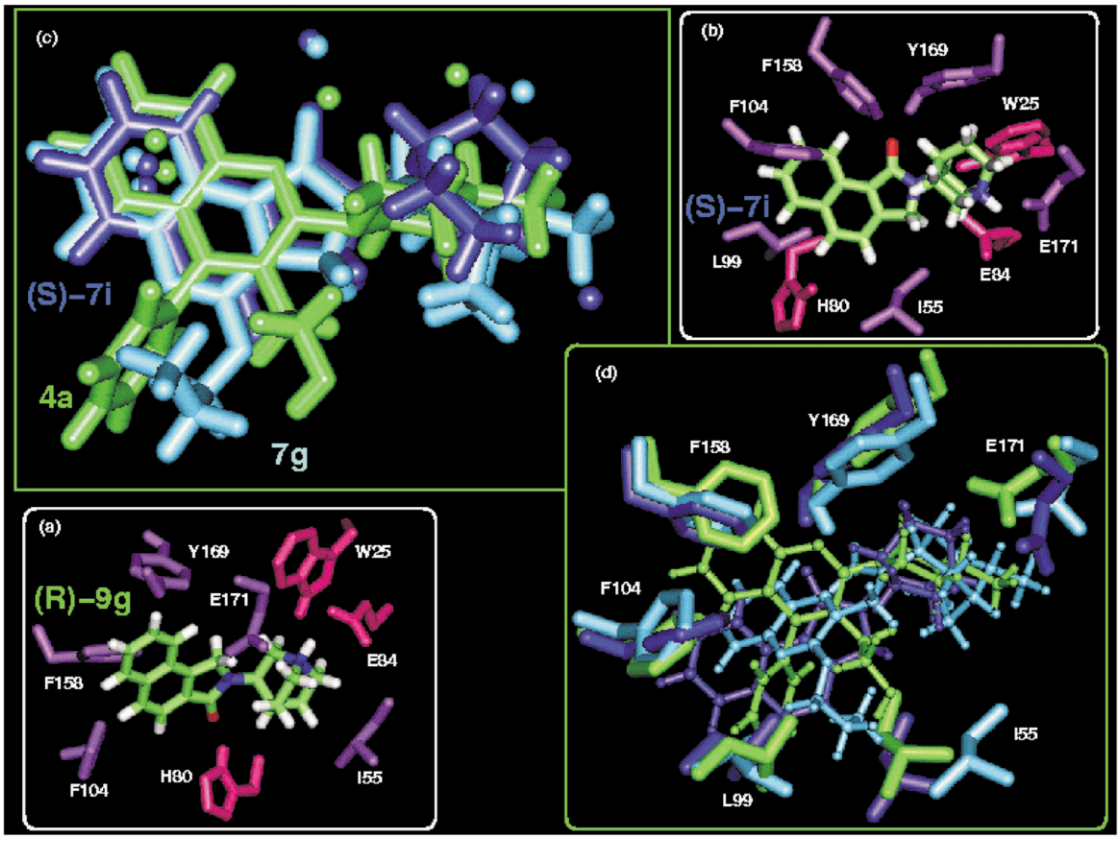

Figure 3. Details of agonists (**3a**) and antagonists (**3b**) binding sites as derived by the energy minimized complexes of the 5-HT_3 receptor with ligand (*R*)-**9g** and (*S*)-**7i**, respectively. Aminoacids belonging to the first receptor subunit (analogue to the α_1 subunit in the nAChR) are reported in violet, those belonging to the second subunit (analogue to the γ subunit in the nAChR) in pink. A comparison of the binding hypotheses derived for the antagonists by indirect (c) and direct (d) approaches is also reported.

high binding stereoselectivity of (*R*)-type and two potential H-bond acceptors in their structures. Taken together, these observations strongly suggest the existence of a peculiar binding mode for quinuclidine derivatives showing a binding stereoselectivity of (*R*)-type which could be determined by the interaction of the additional H-bond acceptor with a suitable donor in the receptor binding site, as confirmed by the analysis of the complexes between compounds (*R*)-**8h**, (*R*)-**46**, (*R*)-**47**, and (*R*)-**48** and the $5HT_3$ receptor. Figure 4 shows that a possible binding mode of these compounds involves residues E84 (second subunit) for the main interaction with the protonated nitrogen, as in the case of agonist binding, S117 (first subunit) for the hydrogen bonding interaction with the oxygen atom of the carbonyl moiety, while Y169 (first subunit), characteristic of the antagonist hydrogen bonding interaction, is invoked here for the interaction with the second hydrogen bonding acceptor site. However, these issues appear to be complicated by the observation that the preferential recognition of (*R*)-enantiomer of **8g** is not accompanied by the presence of two H-bond acceptors.

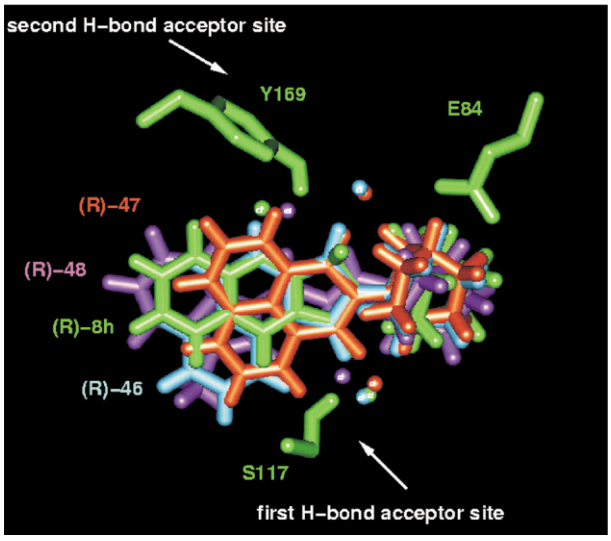

Figure 4. Superposition of quinuclidine 5-HT_3 receptor ligands showing preferential recognition of (*R*) enantiomer: (*R*)-**8h**, (*R*)-**46**, (*R*)-**47**, and (*R*)-**48.** They are represented in interaction with the receptor site, as derived by energy minimization of the complexes. Dummy atoms (d) are used to highlight the hydrogen bonding interactions; they are in fact positioned at 3 Å from the oxygen atom on the lone pair bisector line, and at 3 Å from the nitrogen on the lone pair direction.

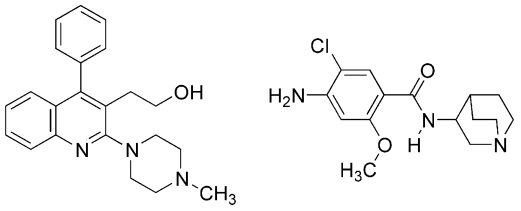

4a

zacopride (**45**)
(*S*)-**45** K_i = 0.2 nM
(*R*)-**45** K_i = 2.6 nM

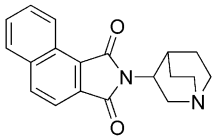

(*S*)-**46** K_i = 119 nM
(*R*)-**46** K_i = 6 nM

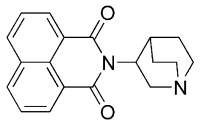

(*S*)-**47** K_i = 61 nM
(*R*)-**47** K_i = 0.9 nM

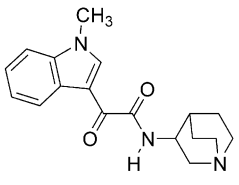

(*S*)-**48** K_i = 13 nM
(*R*)-**48** K_i = 0.25 nM

Chart 2.

Conclusions

A novel class of conformationally constrained derivatives of the classical 5-HT_3 receptor antagonists was developed with the aim of probing the central 5-HT_3 receptor recognition site in a systematic way. Several representatives of this class revealed to be potent 5-HT_3 receptor ligands with affinities in the low nanomolar range. The most potent ligand was quinuclidine derivative (*S*)-**7i**, which showed a subnanomolar affinity comparable with that of the reference ligand granisetron.

The selected tropane derivatives tested in vitro on the 5-HT_3 receptor-dependent [^{14}C]guanidinium uptake in NG 108-15 cells (**7a** and **9a**) were found to behave as potent antagonists, while the quinuclidine derivatives studied showed a whole range of intrinsic efficacies. Thus, the functional behavior of these 5-HT_3 receptor ligands appears to be affected by the structural features of both the azabicyclo moiety and the heteroaromatic portion. In agreement with the data obtained on NG 108-15 cells, investigations on the 5-HT_3 receptor-dependent Bezold–Jarisch reflex in urethane-anesthetized rats confirmed the 5-HT_3 receptor antagonist properties of compounds **7a** and (*S*)-**7i**. Moreover, compounds **7a**, (*S*)-**7i** and **9a** prevented scopolamine-induced amnesia in the mouse passive avoidance test, suggesting a potential usefulness in cognitive disorders for these compounds. Finally, qualitative and quantitative structure-affinity relationship studies derived by an indirect approach were found to be useful in the capturing of information relevant to ligand–receptor interactions. The models obtained corroborate the previous pharmacophoric hypotheses for arylpiperazine[8] and quinuclidine[9] ligands and extended them to the tropane derivatives. However, in spite of the main differences in the binding modes of stereoselective ligands are taken into account in the supermolecule considered (sup-2), the intrinsic limits of the indirect approach, that is the assumption that the ligands considered obey to the same binding paradigm, prevent the rationalization of the binding stereoselectivity. Furthermore, the comparison of the results obtained from the indirect and direct

approaches shows that the alignment criteria normally used in the indirect approach involving a supermolecule as a negative binding site volume are very severe with respect to those imposed by the receptor framework.

Moreover, interesting insights into the interaction mechanism are obtained by the direct approach Different binding modalities seem to characterize the binding of the ligands within the binding crevice as a function of their functional profile and stereosectivity. In particular, the results obtained suggest that the binding of agonists and antagonists differs mainly for the negatively charged aminoacids they chose as counterions. In fact, due to the topography of the interface crevice, the cationic head of the ligands might give rise to a resonant dynamic interaction with two glutamate residues. Competitive antagonists bind preferentially to E171 in the first subunit (corresponding to subunit α1, in the nAChR model), while agonists interact with E84 in the second subunit (corresponding to subunit γ, in the nAChR model) triggering the conformational equilibrium which involves P90, and culminates in the opening of the channel. Partial agonist (*R*)-**8h** is hypothesized to share the same main interaction with E84, but to achieve binding stereoselectivity by interacting with residues of the first subunit. The complexity of the binding paradigm derived is in line with the experimental evidence provided for the nACh receptor[42] which shows that the rapid equilibrium among several functional states of the receptor is affected by reversibly binding ligand and different states of the receptor are characterized by a different structure of the binding site. Obviously alternative hypothesis can be made, however, only additional point mutation data will be able to provide evidence on the reliability of the different binding paradigms proposed.

Experimental

Melting points were determined in open capillaries on a Gallenkamp apparatus and are uncorrected. Microanalyses were carried out by means of a Perkin-Elmer 240C or a Perkin-Elmer Series II CHNS/O Analyzer 2400. Merck silica gel 60 (70–230 or 230–400 mesh) and Merck aluminum oxide 90 II-III, 70–230 mesh, were used for column chromatography. Merck TLC plates, silica gel 60 F_{254}, were used for TLC. ^{1}H NMR spectra were recorded by means of a Bruker AC 200 spectrometer in the indicated solvents (TMS as internal standard): the values of chemical shifts are expressed in ppm and coupling constants (*J*) in Hz. Mass spectra (EI, 70 eV) were recorded either on a VG 70-250S spectrometer (Centro di Analisi e Determinazioni Strutturali, Università di Siena) or a Varian Saturn 3 (Dipartimento Farmaco Chimico Tecnologico, Università di Siena). Optical rotations were measured on a photoelectric Jasco DIP-1000 polarimeter (0.5 dm cell).

General procedure for the bromination of *ortho*-methyl-substituted esters 10, 11a,c–g, 12a,c–e, 13a–f, 28, and 33

A mixture of the appropriate ester (1.5 mmol) in 30 mL of CCl_4 with *N*-bromosuccinimide (0.27 g, 1.5 mmol) and dibenzoyl peroxide (0.03 g, 0.12 mmol) was refluxed under argon for a suitable time, and the reaction progress was monitored by TLC. The solvent was then removed under reduced pressure and the residue was diluted with a small portion of the same solvent. The insoluble succinimide was filtered-off and the solvent was removed under reduced pressure. In most cases the resulting residue was used without further purification, while in some instances purification by flash chromatography was performed before the following reaction was carried out.

Ethyl 2-(bromomethyl)benzoate (14). The title compound was prepared from commercial ethyl 2-methylbenzoate (**10**) (obtained from Aldrich) (reaction time 20 h) and was used without further purification. ^{1}H NMR ($CDCl_3$): 1.43 (t, $J=7.3$, 3H), 4.42 (q, $J=7.2$, 2H), 4.96 (s, 2H), 7.33–7.54 (m, 3H), 7.97 (d, $J=7.7$, 1H).

Ethyl 2-(bromomethyl)-1-naphthalenecarboxylate (15a). The title compound was prepared from ethyl 2-methyl-1-naphthalenecarboxylate (**11a**)[13] (reaction time 2 h and 30 min) and was used without further purification. ^{1}H NMR ($CDCl_3$): 1.50 (t, $J=7.4$, 3H), 4.58 (q, $J=7.4$, 2H), 4.70 (s, 2H), 7.51 (m, 3H), 7.88 (m, 3H).

Methyl 3-(bromomethyl)-2-methoxy-4-quinolinecarboxylate (15e). The title compound was prepared from methyl 2-methoxy-3-methyl-4-quinolinecarboxylate (**11e**) (reaction time 2 h and 30 min) and was used without further purification. ^{1}H NMR ($CDCl_3$): 4.10 (s, 3H), 4.16 (s, 3H), 4.64 (s, 2H), 7.41 (t, $J=7.1$, 1H), 7.66 (m, 2H), 7.86 (d, $J=8.3$, 1H).

Ethyl 3-(bromomethyl)-1,2-dihydro-2-oxo-1-(*n*-propyl)-4-quinolinecarboxylate (29). The title compound was prepared from ethyl 1,2-dihydro-2-oxo-3-methyl-1-(*n*-propyl)-4-quinolinecarboxylate (**28**) (reaction time 2 h and 30 min) and was used without further purification. ^{1}H NMR ($CDCl_3$): 1.06 (t, $J=7.4$, 3H), 1.49 (t, $J=7.0$, 3H), 1.77 (m, 2H), 4.30 (m, 2H), 4.58 (m, 4H), 7.26 (t, $J=7.3$, 1H), 7.37 (d, $J=8.4$, 1H), 7.51–7.64 (m, 2H).

Ethyl 3-(bromomethyl)-2-naphthalenecarboxylate (16a). The title compound was prepared from ethyl 3-methyl-2-naphthalenecarboxylate (**12a**) (reaction time 2 h and 30 min) and was used without further purification. ^{1}H NMR ($CDCl_3$): 1.47 (t, $J=7.0$, 3H), 4.47 (q, $J=7.0$, 2H), 5.13 (s, 2H), 7.44 (m, 2H), 7.81–7.93 (m, 3H), 8.52 (s, 1H).

Ethyl 2-(bromomethyl)-4-chloro-3-quinolinecarboxylate (16c). The title compound was prepared from ethyl 4-chloro-2-methyl-3-quinolinecarboxylate (**12c**) (reaction time 22 h) and was purified by flash chromatography with *n*-hexane–ethyl acetate (8:2) as the eluent (yield 34%). ^{1}H NMR ($CDCl_3$): 1.48 (t, $J=7.3$, 3H), 4.56 (q, $J=7.0$, 2H), 4.80 (s, 2H), 7.69 (t, $J=7.1$, 1H), 7.83 (m, 1H), 8.08 (d, $J=8.7$, 1H), 8.27 (m, 1H).

Ethyl 1-(bromomethyl)-2-naphthalenecarboxylate (17a). The title compound was prepared from ethyl 1-methyl-

2-naphthalenecarboxylate (**13a**) (reaction time 2 h and 45 min) and was used without further purification. ^{1}H NMR ($CDCl_3$): 1.46 (t, $J=7.3$, 3H), 4.46 (q, $J=7.2$, 2H), 5.43 (s, 2H), 7.63 (m, 2H), 7.88 (m, 3H), 8.30 (d, $J=8.6$, 1H).

General procedure for the synthesis of tropane derivatives 6a,b, 7a,c–g, 8a–e, 9a-f, 30, and 35

A mixture of the appropriate γ-haloester (ca. 1.5 mmol) in 30 mL of absolute EtOH with 0.63 g (4.5 mmol) of *endo*-3-aminotropane (*endo*-8-methyl-8-azabicyclo [3.2.1]oct-3-ylamine)[12] (the *exo*-isomer was used for the preparation of compound **6b**) was refluxed under argon for a suitable time, and the reaction progress was monitored by TLC. The solvent was then removed under reduced pressure and the residue was partitioned between ice-cooled water and $CHCl_3$. The organic phase was washed with water, dried over sodium sulfate and concentrated under reduced pressure. In most cases the resulting residue was purified by flash chromatography with ethyl acetate–triethylamine (8:2) as the eluent to obtain the expected tropane derivative, while in some instances recrystallization or washing with a suitable solvent were found to be more appropriate.

***endo*-2-(8-Methyl-8-azabicyclo[3.2.1]oct-3-yl)-2,3-dihydro-1*H*-isoindol-1-one (6a).** This compound was prepared from crude γ-bromoester **14** (reaction time 7 h) and was purified by flash chromatography (yield over two steps: 44%; mp 181–182 °C). ^{1}H NMR ($CDCl_3$): 1.44–1.71 (m, 4H), 2.13–2.23 (m, 5H), 2.36–2.54 (m, 2H), 3.28 (m, 2H), 4.32 (s, 2H), 4.60 (m, 1H), 7.39–7.54 (m, 3H), 7.82 (m, 1H). Anal. ($C_{16}H_{20}N_2O$) C, H, N.

***exo*-2-(8-Methyl-8-azabicyclo[3.2.1]oct-3-yl)-2,3-dihydro-1*H*-isoindol-1-one (6b).** This compound was prepared from crude γ-bromoester **14** (reaction time 8 h) and was purified by flash chromatography with ethyl acetate–methanol–triethylamine (6:2:2) as the eluent (yield over two steps: 41%, mp 179 °C dec). ^{1}H NMR ($CDCl_3$): 1.83 (m, 2H), 2.06–2.28 (m, 4H), 2.57 (m, 5H), 3.61 (br s, 2H), 4.48 (s, 2H), 4.76 (m, 1H), 7.40–7.59 (m, 3H), 7.83 (d, $J=7.0$, 1H). HR-MS: *m*/*z* calcd for ($C_{16}H_{20}N_2O$) 256.1576, found 256.1600. Anal. ($C_{16}H_{20}N_2O$) C, H, N.

***endo*-2-(8-Methyl-8-azabicyclo[3.2.1]oct-3-yl)-2,3-dihydro-1*H*-benz[*e*]isoindol-1-one (7a).** This compound was prepared from crude γ-bromoester **15a** (reaction time 6 h) and was purified by flash chromatography (yield over two steps: 45%). An analytical sample was obtained by recrystallization from ethyl acetate: mp 174–175 °C. ^{1}H NMR ($CDCl_3$): 1.54–1.68 (m, 4H), 2.15–2.24 (m, 5H), 2.44–2.60 (m, 2H), 3.28 (m, 2H), 4.41 (s, 2H), 4.64 (m, 1H), 7.47–7.67 (m, 3H), 7.90 (d, $J=7.6$, 1H), 7.97 (d, $J=8.3$, 1H), 9.24 (d, $J=8.4$, 1H). Anal. ($C_{20}H_{22}N_2O$) C, H, N.

***endo*-2-(8-Methyl-8-azabicyclo[3.2.1]oct-3-yl)-2,3-dihydro-1*H*-pyrrolo[3,4-*c*]quinolin-1-one (7c).** This compound was prepared from crude γ-bromoester **15c** (reaction time 5 h) and was purified by flash chromatography (yield over two steps: 32%; mp 153–154 °C). ^{1}H NMR ($CDCl_3$): 1.50–1.65 (m, 4H), 2.14–2.21 (m, 5H), 2.42–2.59 (m, 2H), 3.28 (m, 2H), 4.46 (s, 2H), 4.61 (m, 1H), 7.61–7.79 (m, 2H), 8.15 (d, $J=8.4$, 1H), 9.05 (m, 2H). MS: *m*/*z* 307 (M^+, 23). Anal. ($C_{19}H_{21}N_3O{\cdot}0.33\ H_2O$) C, H, N.

A mixture of **7d** (50 mg, 0.15 mmol) in 20 mL of ethanol with triethylamine (1.0 mL) and 20 mg of 10% Pd on carbon was hydrogenated at atmospheric pressure for 45 min. The catalyst was filtered off, and the filtrate was evaporated under reduced pressure. The residue was partitioned between CH_2Cl_2 and a solution of 1% NaOH. The organic layer was washed with brine, dried over sodium sulfate and concentrated under reduced pressure to give 23 mg (yield 50%) of **7c**.

***endo*-2-(8-Methyl-8-azabicyclo[3.2.1]oct-3-yl)-4-chloro-2,3-dihydro-1*H*-pyrrolo[3,4-*c*]quinolin-1-one (7d).** This compound was prepared from crude γ-bromoester **15d** (reaction time 1 h) and was purified by flash chromatography (yield over two steps: 60%). An analytical sample was obtained by recrystallization from *n*-hexane–ethyl acetate: mp 169–170 °C. ^{1}H NMR ($CDCl_3$): 1.47–1.66 (m, 4H), 2.16–2.23 (m, 5H), 2.45–2.60 (m, 2H), 3.29 (m, 2H), 4.41 (s, 2H), 4.67 (m, 1H), 7.64–7.83 (m, 2H), 8.09 (d, $J=8.3$, 1H), 9.04 (d, $J=8.6$, 1H). MS: *m*/*z* 341 (M^+, 17). Anal. ($C_{19}H_{20}ClN_3O$) C, H, N.

***endo*-2-(8-Methyl-8-azabicyclo[3.2.1]oct-3-yl)-2,3-dihydro-4-methoxy-1*H*-pyrrolo[3,4-*c*]quinolin-1-one (7e).** This compound was prepared from crude γ-bromoester **15e** (reaction time 1 h) and was purified by flash chromatography (yield over two steps: 40%). An analytical sample was obtained by recrystallization from *n*-hexane–ethyl acetate: mp 190–191 °C. ^{1}H NMR ($CDCl_3$): 1.48–1.62 (m, 4H), 2.04–2.23 (m, 5H), 2.43–2.58 (m, 2H), 3.27 (m, 2H), 4.14 (s, 3H), 4.34 (s, 2H), 4.62 (m, 1H), 7.48 (t, $J=7.2$, 1H), 7.66 (m, 1H), 7.91 (d, $J=8.4$, 1H), 8.92 (m, 1H). MS: *m*/*z* 337 (M^+, 26). Anal. ($C_{20}H_{23}N_3O_2$) C, H, N.

***endo*-2-(8-Methyl-8-azabicyclo[3.2.1]oct-3-yl)-2,3-dihydro-4-ethoxy-1*H*-pyrrolo[3,4-*c*]quinolin-1-one (7f).** This compound was prepared from crude γ-bromoester **15f** (reaction time 18 h) and was purified by flash chromatography (yield over two steps: 37%). An analytical sample was obtained by recrystallization from *n*-hexane–ethyl acetate: mp 195–198 °C. ^{1}H NMR ($CDCl_3$): 1.43–1.72 (m, 7H), 2.14–2.22 (m, 5H), 2.42–2.57 (m, 2H), 3.26 (m, 2H), 4.32 (s, 2H), 4.54–4.72 (m, 3H), 7.46 (t, $J=7.8$, 1H), 7.63 (m, 1H), 7.88 (d, $J=8.4$, 1H), 8.91 (d, $J=7.8$, 1H). MS: *m*/*z* 351 (M^+, 34). Anal. ($C_{21}H_{25}N_3O_2$) C, H, N.

***endo*-2-(8-Methyl-8-azabicyclo[3.2.1]oct-3-yl)-2,3-dihydro-4-(*n*-propyloxy)-1*H*-pyrrolo[3,4-*c*]quinolin-1-one (7g).** This compound was prepared from crude γ-bromoester **15g** (reaction time 15 h) and was purified by flash chromatography (yield over two steps: 44%). An analytical sample was obtained by recrystallization from *n*-hexane–ethyl acetate: mp 170–171 °C. ^{1}H NMR ($CDCl_3$): 1.08 (t, $J=7.4$, 3H), 1.48–1.67 (m, 4H), 1.80–1.98 (m,

2H), 2.19–2.23 (m, 5H), 2.43–2.58 (m, 2H), 3.28 (m, 2H), 4.33 (s, 2H), 4.50–4.73 (m, 3H), 7.48 (t, $J=7.4$, 1H), 7.65 (t, $J=8.1$, 1H), 7.90 (d, $J=8.3$, 1H), 8.93 (d, $J=9.0$, 1H). Anal. ($C_{22}H_{27}N_3O_2$) C, H, N.

***endo*-2-(8-Methyl-8-azabicyclo[3.2.1]oct-3-yl)-2,3,4,5-tetrahydro-5-(*n*-propyl)-1*H*-pyrrolo[3,4-*c*]quinolin-1,4-dione (30).** This compound was prepared from crude γ-bromoester **29** (reaction time 15 h) and was purified by flash chromatography (yield over two steps: 26%). An analytical sample was obtained by washing with diethyl ether: mp 145–148 °C. ^{1}H NMR ($CDCl_3$): 1.07 (t, $J=7.4$, 3H), 1.45–1.65 (m, 4H), 1.71–1.90 (m, 2H), 2.16–2.23 (m, 5H), 2.42–2.57 (m, 2H), 3.26 (m, 2H), 4.32 (m, 4H), 4.61 (m, 1H), 7.27–7.43 (m, 2H), 7.61 (m, 1H), 8.96 (d, $J=7.7$, 1H). MS: m/z 365 (M^+, 33). Anal. ($C_{22}H_{27}N_3O_2\cdot0.5\ H_2O$) C, H, N.

***endo*-2-(8-Methyl-8-azabicyclo[3.2.1]oct-3-yl)-2,3-dihydro-1*H*-benz[*f*]isoindol-1-one (8a).** This compound was prepared from crude γ-bromoester **16a** (reaction time 20 h) and was purified by flash chromatography (yield over two steps: 30%). An analytical sample was obtained by recrystallization from ethyl acetate: mp 217–218 °C. ^{1}H NMR ($CDCl_3$): 1.48–1.66 (m, 4H), 2.15–2.24 (m, 5H), 2.42–2.58 (m, 2H), 3.27 (m, 2H), 4.47 (s, 2H), 4.68 (m, 1H), 7.47–7.59 (m, 2H), 7.84–7.90 (m, 2H), 7.96–8.01 (m, 1H), 8.32 (s, 1H). MS: m/z 306 (M^+, 18). Anal. ($C_{20}H_{22}N_2O\cdot0.25\ H_2O$) C, H, N.

***endo*-2-(8-Methyl-8-azabicyclo[3.2.1]oct-3-yl)-2,3-dihydro-1*H*-pyrrolo[3,4-*b*]quinolin-1-one (8b).** This compound was prepared from ethyl 2-chloromethyl-3-quinolinecarboxylate (**16b**)[18] (reaction time 25 h) and was purified by flash chromatography (yield 51%). An analytical sample was obtained by recrystallization from ethyl acetate: mp 203–204 °C. ^{1}H NMR ($CDCl_3$): 1.47–1.66 (m, 4H), 2.13–2.24 (m, 5H), 2.45–2.60 (m, 2H), 3.28 (m, 2H), 4.52 (s, 2H), 4.75 (m, 1H), 7.61 (t, $J=7.4$, 1H), 7.82 (m, 1H), 7.98 (d, $J=9.0$, 1H), 8.13 (d, $J=8.5$, 1H), 8.57 (s, 1H). Anal. ($C_{19}H_{21}N_3O$) C, H, N.

***endo*-2-(8-Methyl-8-azabicyclo[3.2.1]oct-3-yl)-9-chloro-2,3-dihydro-1*H*-pyrrolo[3,4-*b*]quinolin-1-one (8c).** This compound was prepared from γ-bromoester **16c** (reaction time 2 h) and was purified by flash chromatography (yield 10%; mp 192–193 °C). ^{1}H NMR ($CDCl_3$): 1.56–1.68 (m, 4H), 2.15–2.23 (m, 5H), 2.44–2.59 (m, 2H), 3.27 (m, 2H), 4.47 (s, 2H), 4.62 (m, 1H), 7.69 (t, $J=7.3$, 1H), 7.85 (m, 1H), 8.11 (d, $J=8.3$, 1H), 8.44 (d, $J=8.9$, 1H). MS: m/z 341 (M^+, 10). Anal. ($C_{19}H_{20}ClN_3O\cdot0.2\ H_2O$) C, H, N.

***endo*-2-(8-Methyl-8-azabicyclo[3.2.1]oct-3-yl)-2,3-dihydro-9-methoxy-1*H*-pyrrolo[3,4-*b*]quinolin-1-one (8d).** This compound was prepared from crude γ-bromoester **16d** (reaction time 3 h) and was purified by flash chromatography (yield over two steps: 22%; mp 160–161 °C). ^{1}H NMR ($CDCl_3$): 1.43–1.64 (m, 4H), 2.14–2.23 (m, 5H), 2.42–2.58 (m, 2H), 3.25 (m, 2H), 4.44 (s, 2H), 4.60–4.78 (m, 4H), 7.51 (t, $J=7.2$, 1H), 7.75 (m, 1H), 7.97 (d, $J=8.4$, 1H), 8.35 (d, $J=8.8$, 1H). MS: m/z 337 (M^+, 32). Anal. ($C_{20}H_{23}N_3O_2\cdot0.25\ H_2O$) C, H, N.

***endo*-2-(8-Methyl-8-azabicyclo[3.2.1]oct-3-yl)-2,3-dihydro-9-(*n*-propyloxy)-1*H*-pyrrolo[3,4-*b*]quinolin-1-one (8e).** This compound was prepared from γ-bromoester **16e** (reaction time 8 h) and was purified by flash chromatography (yield 16%; mp 125–126 °C). ^{1}H NMR ($CDCl_3$): 1.09 (t, $J=7.4$, 3H), 1.46–1.66 (m, 4H), 1.82–1.99 (m, 2H), 2.07–2.23 (m, 5H), 2.42–2.57 (m, 2H), 3.25 (m, 2H), 4.43 (s, 2H), 4.71 (m, 1H), 4.95 (t, $J=6.9$, 2H), 7.51 (t, $J=7.2$, 1H), 7.75 (m, 1H), 7.97 (d, $J=8.4$, 1H), 8.39 (m, 1H). MS: m/z 365 (M^+, 24). Anal. ($C_{22}H_{27}N_3O_2\cdot0.33\ H_2O$) C, H, N.

***endo*-2-[8-Methyl-8-azabicyclo[3.2.1]oct-3-yl]-2,3-dihydro-4-(*n*-propyl)-pyrrolo[3,4-*b*]quinolin-1,9(1*H*,4*H*)-dione (35).** This compound was prepared from γ-bromoester **34** (reaction time 22 h) and was purified by washing with diethyl ether (yield 27%). An analytical sample was obtained by recrystallization from ethanol–ethyl acetate: mp 198 °C dec. ^{1}H NMR ($CDCl_3$): 1.08 (t, $J=7.4$, 3H) 1.60–1.80 (m, 4H), 1.84–2.03 (m, 2H), 2.16–2.28 (m, 5H), 2.41–2.56 (m, 2H), 3.32 (m, 2H), 4.02 (t, $J=7.8$, 2H), 4.29 (s, 2H), 4.46 (m, 1H), 7.34–7.43 (m, 2H), 7.60–7.69 (m, 1H), 8.49–8.54 (m, 1H). MS (FAB): m/z 366 ($M+1$, 100). Anal. ($C_{22}H_{27}N_3O_2$) C, H, N.

***endo*-2-(8-Methyl-8-azabicyclo[3.2.1]oct-3-yl)-1,2-dihydro-3*H*-benz[*e*]isoindol-3-one (9a).** This compound was prepared from crude γ-bromoester **17a** (reaction time 17 h) and was purified by flash chromatography (yield over two steps: 52%). An analytical sample was obtained by recrystallization from ethyl acetate: mp 139–140 °C. ^{1}H NMR ($CDCl_3$): 1.52–1.69 (m, 4H), 2.16–2.24 (m, 5H), 2.44–2.60 (m, 2H), 3.29 (m, 2H), 4.58–4.75 (m, 3H), 7.54–7.62 (m, 2H), 7.80–7.99 (m, 4H). MS: m/z 306 (M^+, 9). Anal. ($C_{20}H_{22}N_2O$) C, H, N.

***endo*-2-(8-Methyl-8-azabicyclo[3.2.1]oct-3-yl)-1,2-dihydro-3*H*-pyrrolo[3,4-*c*]quinolin-3-one (9b).** This compound was prepared from crude γ-bromoester **17b** (reaction time 15 h) and was purified by washing with diethyl ether (yield over two steps: 45%; mp 195–196 °C). ^{1}H NMR ($CDCl_3$): 1.49–1.68 (m, 4H), 2.18–2.24 (m, 5H), 2.45–2.60 (m, 2H), 3.30 (m, 2H), 4.59–4.73 (m, 3H), 7.65 (t, $J=7.3$, 1H), 7.78–7.91 (m, 2H), 8.23 (d, $J=8.4$, 1H), 9.27 (s, 1H). MS: m/z 307 (M^+, 10). Anal. ($C_{19}H_{21}N_3O\cdot0.25\ H_2O$) C, H, N.

***endo*-2-(8-Methyl-8-azabicyclo[3.2.1]oct-3-yl)-4-chloro-1,2-dihydro-3*H*-pyrrolo[3,4-*c*]quinolin-3-one (9c).** This compound was prepared from crude γ-bromoester **17c** (reaction time 5 h) and was purified by washing with diethyl ether (yield over two steps: 73%; mp 229–231 °C. ^{1}H NMR ($CDCl_3$): 1.58–1.70 (m, 4H), 2.16–2.23 (m, 5H), 2.43–2.58 (m, 2H), 3.29 (m, 2H), 4.55 (m, 1H), 4.65 (s, 2H), 7.65 (t, $J=7.7$, 1H), 7.79–7.88 (m, 2H), 8.12 (d, $J=8.6$, 1H). MS: m/z 341 (M^+, 35). Anal. ($C_{19}H_{20}ClN_3O\cdot0.25\ H_2O$) C, H, N.

***endo*-2-(8-Methyl-8-azabicyclo[3.2.1]oct-3-yl)-1,2-dihydro-4-methoxy-3*H*-pyrrolo[3,4-*c*]quinolin-3-one (9d).** This compound was prepared from crude γ-bromoester **17d** (reaction time 2 h) and was purified by recrystallization from ethyl acetate (yield over two steps: 48%; mp 179–

180 °C). ^{1}H NMR ($CDCl_3$): 1.55–1.68 (m, 4H), 2.14–2.22 (m, 5H), 2.40–2.55 (m, 2H), 3.26 (m, 2H), 4.18 (s, 3H), 4.50 (m, 1H), 4.59 (s, 2H), 7.43 (t, $J=7.4$, 1H), 7.65–7.76 (m, 2H), 7.91 (d, $J=8.3$, 1H). MS: m/z 337 (M^+, 36). Anal. ($C_{20}H_{23}N_3O_2\cdot0.66\ H_2O$) C, H, N.

***endo*-2-(8-Methyl-8-azabicyclo[3.2.1]oct-3-yl)-1,2-dihydro-4-ethoxy-3*H*-pyrrolo[3,4-*c*]quinolin-3-one (9e).** This compound was prepared from crude γ-bromoester **17e** (reaction time 2 h) and was purified by flash chromatography (yield over two steps: 27%). An analytical sample was obtained by washing with diethyl ether: mp 169–170 °C. ^{1}H NMR ($CDCl_3$): 1.48–1.68 (m, 7H), 2.13–2.22 (m, 5H), 2.39–2.55 (m, 2H), 3.26 (m, 2H), 4.48 (m, 1H), 4.59 (s, 2H), 4.67 (q, $J=7.0$, 2H), 7.42 (t, $J=7.8$, 1H), 7.63–7.75 (m, 2H), 7.88 (d, $J=8.4$, 1H). MS: m/z 351 (M^+, 31). Anal. ($C_{21}H_{25}N_3O_2\cdot0.2\ H_2O$) C, H, N.

***endo*-2-(8-Methyl-8-azabicyclo[3.2.1]oct-3-yl)-1,2-dihydro-4-(*n*-propyloxy)-3*H*-pyrrolo[3,4-*c*]quinolin-3-one (9f).** This compound was prepared from crude γ-bromoester **17f** (reaction time 3 h) and was purified by flash chromatography (yield over two steps: 19%; mp 153–155 °C. ^{1}H NMR ($CDCl_3$): 1.08 (t, $J=7.4$, 3H), 1.56–1.68 (m, 4H), 1.85–2.03 (m, 2H), 2.14–2.23 (m, 5H), 2.40–2.55 (m, 2H), 3.26 (m, 2H), 4.43–4.59 (m, 5H), 7.41 (t, $J=7.3$, 1H), 7.64–7.75 (m, 2H), 7.88 (d, $J=8.4$, 1H). MS: m/z 365 (M^+, 32). Anal. ($C_{22}H_{27}N_3O_2\cdot0.25\ H_2O$) C, H, N.

***endo*-2-(8-Azabicyclo[3.2.1]oct-3-yl)-2,3-dihydro-1*H*-benz[*e*]isoindol-1-one (7b).** A mixture of **7a** (0.11 g, 0.36 mmol) in 1 mL (9.3 mmol) of α-chloroethyl chloroformate (ACE-Cl)[43] was heated for 3 h at 100 °C under argon. Excess ACE-Cl was then removed under reduced pressure, and methanol was added to the residue. The resulting mixture was heated at reflux for 20 min and concentrated to dryness. The residue obtained was washed with ethyl acetate–methanol and partitioned between CH_2Cl_2 and a solution of 1% NaOH. The organic layer was washed with brine, dried over sodium sulfate and concentrated under reduced pressure to give pure **7b** (72 mg, yield 68%, mp 142–143 °C). ^{1}H NMR ($CDCl_3$): 1.46–1.91 (m, 7H), 2.35–2.46 (m, 2H), 3.68 (m, 2H), 4.38 (s, 2H), 4.58 (m, 1H), 7.46–7.67 (m, 3H), 7.89 (d, $J=7.8$, 1H), 7.96 (d, $J=8.4$, 1H), 9.22 (d, $J=8.2$, 1H). MS: m/z 292 (M^+, 13). Anal. ($C_{19}H_{20}N_2O\cdot0.2\ H_2O$) C, H, N.

***endo*-2-(8-Methyl-8-azabyciclo[3.2.1]oct-3-yl]-2,3-dihydro-4-hydroxy-1*H*-pyrrolo[3,4-*c*]quinolin-1-one (7h).** A solution of **7d** (85 mg, 0.25 mmol) in 15 mL of 1 N HCl was heated for 4 h at 80 °C. The resulting reaction mixture was cooled at 0–5 °C, made alkaline (pH 9) with 3 N NaOH and extracted with chloroform. The combined organic extracts were dried over sodium sulfate and concentrated under reduced pressure to give 71 mg of **7h** (yield 88%). An analytical sample was obtained by recrystallization from ethyl acetate; mp 246 °C dec. ^{1}H NMR ($CDCl_3$): 1.46–1.61 (m, 4H), 2.16–2.23 (m, 5H), 2.43–2.58 (m, 2H), 3.27 (m, 2H), 4.35 (s, 2H), 4.61 (m, 1H), 7.28–7.36 (m, 2H), 7.55 (m, 1H), 8.84 (d, $J=8.2$, 1H), 10.63 (br s, 1H). MS: m/z 323 (M^+, 28). Anal. ($C_{19}H_{21}N_3O_2\cdot0.33\ H_2O$) C, H, N.

***endo,cis*-2-(8-Methyl-8-azabicyclo[3.2.1]oct-3-yl)-2,3,3a,4,5,9b-hexahydro-1*H*-pyrrolo[3,4-*c*]quinolin-1-one (18).** A mixture of **7d** (0.10 g, 0.29 mmol) in 30 mL of ethanol with triethylamine (1.5 mL) and 45 mg of 10% Pd on carbon was hydrogenated at 50 psi for 1 h and 15 min. The catalyst was filtered off, and the filtrate was evaporated under reduced pressure. The residue was partitioned between CH_2Cl_2 and a solution of 1% NaOH. The organic layer was washed with brine, dried over sodium sulfate and concentrated under reduced pressure. Recrystallization of the residue from *n*-hexane–ethyl acetate gave 21 mg (yield 23%) of **18** as colorless prisms melting at 191–192 °C. ^{1}H NMR ($CDCl_3$): 1.25–1.57 (m, 4H), 2.06–2.39 (m, 7H), 2.77–2.95 (m, 2H), 3.08–3.28 (m, 4H), 3.51 (m, 2H), 3.76 (br s, 1H), 4.24 (m, 1H), 6.54 (d, $J=7.9$, 1H), 6.76 (t, $J=7.4$, 1H), 7.02 (t, $J=7.8$, 1H), 7.50 (d, $J=7.6$, 1H). MS: m/z 311 (M^+, 27). Anal. ($C_{19}H_{25}N_3O$) C, H, N.

***endo*-2-(8-Methyl-8-azabicyclo[3.2.1]oct-3-yl)-2,3-dihydro-9-hydroxy-1*H*-pyrrolo[3,4-*b*]quinolin-1-one (8f).** A solution of **8c** (63 mg, 0.18 mmol) in 15 mL of 1 N HCl was heated for 23 h at 80 °C, then cooled at 0–5 °C, and made alkaline (pH 9) with 3 N NaOH. The precipitate was collected by filtration, dried and purified by recrystallization from ethyl acetate–ethanol to give 25 mg of **8f** (yield 43%; mp 228 °C dec). ^{1}H NMR (CD_3OD): 1.85–2.24 (m, 6H), 2.35–2.48 (m, 5H), 3.52 (m, 2H), 4.32 (m, 1H), 4.48 (s, 2H), 7.36 (m, 1H), 7.69 (m, 2H), 8.36 (d, $J=8.0$, 1H). MS(FAB): m/z 324 ($M+1$, 7). Anal. ($C_{19}H_{21}N_3O_2\cdot7\ H_2O$) C, H, N.

Ethyl 3-methyl-2-naphthalenecarboxylate (12a). A mixture of **23**[15] (1.0 g, 2.9 mmol) in 20 mL of anhydrous DMF with LiCl (0.61 g, 14.4 mmol) and Me_4Sn (0.40 mL, 2.9 mmol) was stirred at room temperature under argon for 15 min and was added $Pd(PPh_3)_2Cl_2$ (0.1 g, 0.14 mmol). The resulting mixture was heated at 120–130 °C under argon while 1.0 mL (7.2 mmol) of Me_4Sn was added in 15 min. After the addition was completed, the heating was continued for additional 30 min. The solvent was then removed under reduced pressure, and the residue was partitioned between CH_2Cl_2 and water. The organic layer was dried over sodium sulfate, and concentrated under reduced pressure. Purification of the residue by flash chromatography with CH_2Cl_2 as the eluent gave 0.56 g of **12a** (yield 90%) as a white crystalline solid: mp 47–48 °C (lit.[44] mp 45–46 °C).^{1}H NMR ($CDCl_3$): 1.44 (t, $J=7.3$, 3H), 2.73 (s, 3H), 4.42 (q, $J=7.2$, 2H), 7.49 (m, 2H), 7.66 (s, 1H), 7.76 (d, $J=8.0$, 1H), 7.87 (d, $J=7.9$, 1H), 8.47 (s, 1H). MS: m/z 214 (M^+, 100).

Ethyl 1-methyl-2-naphthalenecarboxylate (13a). This compound was prepared in 91% yield from **24** by means of the same procedure described for **12a**.^{1}H NMR ($CDCl_3$): 1.43 (t, $J=7.2$, 3H), 2.92 (s, 3H), 4.42 (q, $J=7.0$, 2H), 7.56 (m, 2H), 7.68–7.86 (m, 3H), 8.18 (m, 1H) (in agreement with that described by Maeyama et al.[45]). MS: m/z 214 (M^+, 100).

2-Chloro-3-methyl-4-quinolinecarboxylic acid chloride (27). A mixture of acid **25**[16] (1.3 g, 6.4 mmol) in $POCl_3$ (10 mL) was refluxed for 45 min under argon. Then, the cooled reaction mixture was poured into ice-water and the precipitate was extracted with $CHCl_3$. The combined extracts were dried over sodium sulfate and evaporated under reduced pressure. The residue was purified by flash chromatography with *n*-hexane–ethyl acetate (8:2) as the eluent to give 1.4 g of **27** as colorless crystals (yield 91%; mp 51–52 °C; lit.[46] mp 52 °C). ^{1}H NMR ($CDCl_3$): 2.60 (s, 3H), 7.68 (m, 1H), 7.74–7.80 (m, 2H), 8.06 (m, 1H). MS: *m*/*z* 239 (M^+, 24). Anal. ($C_{11}H_7Cl_2NO$) C, H, N.

Ethyl 3-methyl-2-(*n*-propyloxy)-4-quinolinecarboxylate (11g). To a solution of **26** (0.70 g, 3.0 mmol) in 15 mL of anhydrous DMF was added NaH (84 mg, 3.5 mmol) and the resulting mixture was stirred at room temperature for 20 min under argon. Then, propyl iodide (0.35 mL, 3.5 mmol) was added dropwise and the reaction mixture was stirred at room temperature for 2 h and 30 min. After the reaction was completed, the mixture was poured into ice-water and extracted with CH_2Cl_2. The combined extracts were washed with water, dried over sodium sulfate and evaporated under reduced pressure. Purification of the residue by flash chromatography with *n*-hexane–ethyl acetate (8:2) as the eluent gave 0.16 g of **11g** as the less polar fraction (yield 19%). ^{1}H NMR ($CDCl_3$): 1.07 (t, J = 7.4, 3H), 1.46 (t, J = 7.4, 3H), 1.87 (m, 2H), 2.32 (s, 3H), 4.42–4.59 (m, 4H), 7.36 (t, J = 7.3, 1H), 7.58 (m, 2H), 7.80 (d, J = 8.3, 1H).

Ethyl 1,2-dihydro-3-methyl-2-oxo-1-(*n*-propyl)-4-quinolinecarboxylate (28). The title compound was separated as the more polar fraction during the purification by chromatography of compound **11g**. Compound **28** (0.42 g, yield 51%) was obtained as a white solid melting at 81–83 °C. ^{1}H NMR ($CDCl_3$): 1.05 (t, J = 7.4, 3H), 1.45 (t, J = 7.4, 3H), 1.78 (m, 2H), 2.24 (s, 3H), 4.28 (m, 2H), 4.52 (q, J = 7.0, 2H), 7.19 (m, 1H), 7.33–7.57 (m, 3H).

General procedure for the synthesis of alkoxyquinoline derivatives 11e,f, 12d, and 13d,e

To a solution of the appropriate chloroderivative (**27**, **12c**, or **13c**) (2.1 mmol) in 20 mL of anhydrous methanol (or ethanol) cooled at 0–5 °C was added portionwise NaH (0.15 g, 6.2 mmol). The resulting mixture was stirred at room temperature for 1 h under argon and refluxed for 4–16 h. Then, the solvent was removed under reduced pressure and the residue was partitioned between ice-cooled water and $CHCl_3$. The organic layer was dried over sodium sulfate, and concentrated under reduced pressure. Purification of the residue by flash chromatography with *n*-hexane–ethyl acetate (8:2) as the eluent gave the expected alkoxyquinoline derivative.

Methyl 2-methoxy-3-methyl-4-quinolinecarboxylate (11e). Title compound was obtained from **27** (yield 91%) as a colorless oil which crystallized on standing: mp 59–61 °C. ^{1}H NMR ($CDCl_3$): 2.30 (s, 3H), 4.04 (s, 3H), 4.10 (s, 3H), 7.36 (m, 1H), 7.57 (m, 2H), 7.84 (d, J = 8.2, 1H).

Ethyl 2-ethoxy-3-methyl-4-quinolinecarboxylate (11f). This compound was prepared from **27** (yield 79%) as a pale yellow oil. ^{1}H NMR ($CDCl_3$): 1.45 (t, J = 7.0, 6H), 2.30 (s, 3H), 4.48–4.59 (m, 4H), 7.36 (m, 1H), 7.58 (m, 2H), 7.80 (d, J = 8.4, 1H).

Ethyl 2-chloro-3-methyl-4-quinolinecarboxylate (11d). A mixture of **27** (0.24 g, 1.0 mmol) in 25 mL of absolute ethanol and 0.28 mL (2.0 mmol) of triethylamine was refluxed for 40 min, concentrated under reduced pressure and partitioned between CH_2Cl_2 and water. The organic layer was dried over sodium sulfate, and concentrated under reduced pressure. Purification of the residue by flash chromatography with *n*-hexane–ethyl acetate (8:2) as the eluent gave 0.23 g of **11d** as a white crystalline solid (yield 92%, mp 53–54 °C). ^{1}H NMR ($CDCl_3$): 1.46 (t, J = 7.0, 3H), 2.51 (s, 3H), 4.57 (q, J = 7.1, 2H), 7.55 (m, 1H), 7.69 (m, 2H), 7.99 (d, J = 8.3, 1H). MS: *m*/*z* 249 (M^+, 38).

Ethyl 3-Methyl-4-quinolinecarboxylate (11c). A mixture of **11d** (0.29 g, 1.2 mmol) in 20 mL of ethanol with triethylamine (0.5 mL) and 0.15 g of 10% Pd on carbon was hydrogenated for 35 min at atmospheric pressure and room temperature. The catalyst was filtered off, and the filtrate was evaporated under reduced pressure. The residue was partitioned between CH_2Cl_2 and water. The organic layer was washed with brine, dried over sodium sulfate and concentrated under reduced pressure. Purification of the residue by flash chromatography with *n*-hexane–ethyl acetate (8:2) as the eluent gave 0.22 g of **11c** as a colorless oil (yield 85%). ^{1}H NMR ($CDCl_3$): 1.46 (t, J = 7.0, 3H), 2.51 (s, 3H), 4.55 (d, J = 7.0, 2H), 7.52–7.72 (m, 2H), 7.81 (d, J = 7.6, 1H), 8.08 (d, J = 8.3, 1H), 8.80 (s, 1H). MS: *m*/*z* 215 (M^+, 78).

Ethyl 4-chloro-2-methyl-3-quinolinecarboxylate (12c). This compound was prepared in 92% yield from **31**[17] by the same procedure described for **27** with the difference that **12c** was extracted at pH 8–9. ^{1}H NMR ($CDCl_3$): 1.44 (t, J = 7.2, 3H), 2.72 (s, 3H), 4.51 (q, J = 7.2, 2H), 7.61 (t, J = 7.2, 1H), 7.77 (m, 1H), 8.02 (d, J = 8.4, 1H), 8.20 (d, J = 7.7, 1H).

Ethyl 2-methyl-4-(*n*-propyloxy)-3-quinolinecarboxylate (12e). This compound was prepared from 1.5 g (6.5 mmol) of ethyl 1,4-dihydro-2-methyl-4-oxo-3-quinolinecarboxylate (**31**)[17] employing the same procedure described for **11g** with the exception that the reaction time was 24 h. Compound **12e** was purified by flash chromatography with CH_2Cl_2–ethyl acetate (8:2) as the eluent (0.95 g, yield 53%). ^{1}H NMR ($CDCl_3$): 1.08 (t, J = 7.4, 3H), 1.43 (t, J = 7.2, 3H), 1.89 (m, 2H), 2.68 (s, 3H), 4.17 (t, J = 6.4, 2H), 4.46 (q, J = 7.0, 2H), 7.48 (t, J = 8.0, 1H), 7.69 (m, 1H), 7.97 (d, J = 8.4, 1H), 8.11 (d, J = 7.9, 1H).

Ethyl 1,4-dihydro-2-methyl-4-oxo-1-(*n*-propyl)-3-quinolinecarboxylate (33). NaH (0.24 g, 10 mmol) was added portionwise to a solution of ethyl acetoacetate (1.3 mL, 10 mmol) in 20 mL of *N*,*N*-dimethylacetamide under stirring at room temperature. To the resulting mixture was added *N*-propylisatoic anhydride (**32**)[47] (2.4 g, 12 mmol) followed by stirring for 10 min at 120 °C. The

solvent was removed under reduced pressure, the residue was treated with ice-water, and extracted with $CHCl_3$. The combined extracts were washed with water, dried over sodium sulfate and evaporated under reduced pressure. Purification of the residue by flash chromatography with CH_2Cl_2–ethyl acetate (1:1) as the eluent gave 1.9 g of **33** (yield 69%). ^{1}H NMR ($CDCl_3$): 1.08 (t, $J=7.5$, 3H), 1.39 (t, $J=6.9$, 3H), 1.85 (m, 2H), 2.51 (s, 3H), 4.09 (m, 2H), 4.42 (q, $J=7.2$, 2H), 7.32–7.45 (m, 2H), 7.64 (m, 1H), 8.45 (m, 1H).

Ethyl 4-methyl-2-(*n*-propyloxy)-3-quinolinecarboxylate (13f). This compound was prepared from 1.0 g (4.3 mmol) of **37**[48] by the same procedure described for **11g**. Compound **13f** was purified by flash chromatography with *n*-hexane–ethyl acetate (8:2) as the eluent (0.21 g, yield 18%). ^{1}H NMR ($CDCl_3$): 1.02 (t, $J=7.4$, 3H), 1.41 (t, $J=7.3$, 3H), 1.81 (m, 2H), 2.59 (s, 3H), 4.45 (m, 4H), 7.40 (t, $J=8.0$, 1H), 7.63 (m, 1H), 7.80 (d, $J=8.7$, 1H), 7.89 (d, $J=8.5$, 1H).

Ethyl 2-chloro-4-methyl-3-quinolinecarboxylate (13c). This compound was prepared from **37**[48] (2.0 g, 8.6 mmol) by the same procedure described for **27** with the difference that **13c** was purified by recrystallization from methanol (1.8 g, yield 84%, mp 109–110 °C). ^{1}H NMR ($CDCl_3$): 1.44 (t, $J=7.3$, 3H), 2.68 (s, 3H), 4.50 (q, $J=7.1$, 2H), 7.61 (m, 1H), 7.76 (m, 1H), 8.01 (m, 2H). MS: m/z 249 (M^+, 38).

Ethyl 4-methyl-3-quinolinecarboxylate (13b). This compound was prepared in 79% yield from **13c** by the same procedure described for **11c** with the difference that the reaction time for **13b** was 4 h. ^{1}H NMR ($CDCl_3$): 1.44 (t, $J=7.0$, 3H), 2.98 (s, 3H), 4.45 (d, $J=7.0$, 2H), 7.61 (t, $J=7.3$, 1H), 7.77 (m, 1H), 8.15 (m, 2H), 9.23 (s, 1H). MS: m/z 215 (M^+, 70).

Inner salt 39. A mixture of 3-aminoquinuclidine dihydrochloride (**38**) (Aldrich) (0.20 g, 1.0 mmol) in absolute ethanol (30 mL) with anhydrous Na_2CO_3 (0.45 g 4.2 mmol) was refluxed for 1 h under argon. A solution of ethyl 2-chloromethyl-3-quinolinecarboxylate (**16b**)[18] (0.25 g, 1.0 mmol) in absolute ethanol (20 mL) was then added to the reaction mixture and the reflux was continued for additional 26 h. The solid material was filtered off and the solvent was removed under reduced pressure to give inner salt **39** as a thick oil (0.30 g, yield 96%) soluble in water and insoluble in apolar solvents. ^{1}H NMR (CD_3OD): 1.87–2.26 (m, 5H), 3.25 (m, 1H), 3.39 (m, 1H), 3.68 (m, 4H), 3.99 (m, 1H), 5.14 (q, $J=12.8$, 2H), 7.65 (t, $J=7.4$, 1H), 7.81 (m, 1H), 7.99 (d, $J=8.0$, 1H), 8.08 (d, $J=8.3$, 1H), 8.73 (s, 1H). MS (FAB): m/z 312 ($M+1$, 100).

General procedure for the synthesis of quinuclidine derivatives 6c, 7i, 8g,h, and 9g

A mixture of 3-aminoquinuclidine dihydrochloride (**38**) [(*RS*), (*S*), or (*R*) available from Aldrich] (0.51 g, 2.56 mmol) in absolute ethanol (30 mL) with anhydrous Na_2CO_3 (1.1 g, 10.4 mmol) was refluxed for 1 h under argon, then cooled at 0–5 °C and 0.21 mL (2.42 mmol) of allyl bromide was added. The resulting reaction mixture was stirred for 15 min at 0–5 °C, for 30 min at room temperature, and heated to reflux for 30 min. A solution of the appropriate γ-haloester (2.52 mmol) in the suitable amount of absolute ethanol (typically 10–20 mL) was then added to the reaction mixture and the reflux was continued until the γ-haloester was transformed as seen by TLC monitorization. The solvent was removed under reduced pressure and the residue was washed with hot anhydrous DMF (3 × 15 mL). The organic phase was treated with dipropylamine (2.0 mL, 14.6 mmol) and $Pd(PPh_3)_2Cl_2$ (0.050 g, 0.071 mmol) and heated at 95–100 °C for 1 h under argon. The reaction mixture was then concentrated under reduced pressure and the residue was partitioned between diethyl ether and 3 N HCl. The aqueous solution was made alkaline with 50% NaOH solution and the precipitate was collected by filtration or extracted with ethyl acetate. The combined extracts were washed with brine, dried over sodium sulfate, and concentrated under reduced pressure. Purification of the residue by washing or recrystallization with the appropriate solvent gave the expected quinuclidine derivative.

2-(1-Azabicyclo[2.2.2]oct-3-yl)-2,3-dihydro-1*H*-isoindol-1-one hydrochloride (6c). This compound was prepared from crude γ-bromoester **14** (reaction time 16 h) and was purified as a HCl salt by washing with acetone (yield over two steps: 38%; mp 217–220 °C). ^{1}H NMR ($CDCl_3$): 1.92–2.33 (m, 4H), 2.52 (m, 1H), 3.37 (m, 3H), 3.78 (m, 2H), 3.99 (m, 1H), 4.49–4.72 (m, 3H), 7.47–7.62 (m, 3H), 7.84 (m, 1H), 12.35 (br s, 1H). HR-MS: m/z calcd for ($C_{15}H_{18}N_2O$) 242.1419, found 242.1418. Anal. ($C_{15}H_{18}N_2O$·HCl.2 H_2O) C, H, N.

2-(1-Azabicyclo[2.2.2]oct-3-yl)-2,3-dihydro-1*H*-benz[*e*]isoindol-1-one (7i). This compound was prepared from crude γ-bromoester **15a** (reaction time 17 h) and was purified as a free base by washing with diethyl ether (yield over two steps: 31%; mp 138–141 °C). ^{1}H NMR ($CDCl_3$): 1.59–1.96 (m, 4H), 2.20 (m, 1H), 2.89–3.18 (m, 5H), 3.41 (m, 1H), 4.48 (t, $J=8.3$, 1H), 4.64 (q, $J=17.7$, 2H), 7.49–7.68 (m, 3H), 7.90 (d, $J=8.1$, 1H), 7.98 (d, $J=8.4$, 1H), 9.20 (d, $J=8.3$, 1H). Anal. ($C_{19}H_{20}N_2O$·0.75 H_2O) C, H, N.

Compound (*S*)-**7i**: yield 32%; mp 152–154 °C; $[\alpha]_D^{24}$ −42.1° (*c* 1.5, methanol). Anal. ($C_{19}H_{20}N_2O$·0.33 H_2O) C, H, N.

Compound (*R*)-**7i**: yield 29%; mp 155–157 °C. $[\alpha]_D^{24}$ +40.0° (*c* 0.5, methanol). Anal. ($C_{19}H_{20}N_2O$) C, H, N.

2-(1-Azabicyclo[2.2.2]oct-3-yl)-2,3-dihydro-1*H*-benz[*f*]isoindol-1-one (8g). This compound was prepared from crude γ-bromoester **16a** (reaction time 6 h) and was purified as a free base by washing with diethyl ether (yield over two steps: 42%; mp 208–210 °C). ^{1}H NMR ($CDCl_3$): 1.59–1.96 (m, 4H), 2.18 (m, 1H), 2.87–3.15 (m, 5H), 3.39 (m, 1H), 4.50 (t, $J=8.2$, 1H), 4.74 (q, $J=15.9$, 2H), 7.50–7.61 (m, 2H), 7.88–7.93 (m, 2H), 8.01 (m, 1H), 8.37 (s, 1H). MS: m/z 292 (M^+, 27). Anal. ($C_{19}H_{20}N_2O$·0.25 H_2O) C, H, N.

Compound (*S*)-**8g**: yield 37%; mp 220–222 °C; $[\alpha]_D^{24}$ −39.5° (*c* 0.4, methanol). Anal. ($C_{19}H_{20}N_2O\cdot 2.5\ H_2O$) C, H, N.

Compound (*R*)-**8g**: yield 42%; mp 220–222 °C. $[\alpha]_D^{24}$ +36.7° (*c* 0.4, methanol). Anal. ($C_{19}H_{20}N_2O\cdot H_2O$) C, H, N.

2-(1-azabicyclo[2.2.2]oct-3-yl)-2,3-dihydro-1*H*-pyrrolo[3,4-*b*]quinolin-1-one (8h). This compound was prepared from γ-chloroester **16b**[18] (reaction time 21 h) and was purified as a free base by recrystallization from ethyl acetate (yield: 35%; mp 207–208 °C). ^{1}H NMR ($CDCl_3$): 1.57–1.96 (m, 4H), 2.20 (m, 1H), 2.88–3.15 (m, 5H), 3.42 (m, 1H), 4.54 (t, *J* = 8.2, 1H), 4.79 (q, *J* = 16.8, 2H), 7.63 (t, *J* = 7.4, 1H), 7.85 (m, 1H), 8.01 (d, *J* = 8.5, 1H), 8.15 (d, *J* = 8.5, 1H), 8.62 (s, 1H). MS: *m*/*z* 293 (M^+, 38). Anal. ($C_{18}H_{19}N_3O$) C, H, N.

Compound (*S*)-**8h**: yield 51%; mp 207–208 °C; $[\alpha]_D^{24}$ −41.2° (*c* 0.3, methanol). Anal. ($C_{18}H_{19}N_3O\cdot 1.5\ H_2O$) C, H, N.

Compound (*R*)-**8h**: yield 43%; mp 207–208 °C. $[\alpha]_D^{24}$ +36.1° (*c* 0.3, methanol). Anal. ($C_{18}H_{19}N_3O\cdot 0.25\ H_2O$) C, H, N.

(*R*)-2-(1-Azabicyclo[2.2.2]oct-3-yl)-1,2-dihydro-3*H*-benz[*e*]isoindol-3-one [(*R*)-9g]. This compound was prepared from crude γ-bromoester **17a** (reaction time 4 h) and was purified as a free base by washing with diethyl ether (yield over two steps: 31%; mp 152–154 °C); $[\alpha]_D^{24}$ +48.2° (*c* 0.3, methanol); $[\alpha]_D^{24}$ +44.6° (*c* 1.0, methanol–diethylamine 9:1). ^{1}H NMR ($CDCl_3$): 1.59–1.97 (m, 4H), 2.20 (m, 1H), 2.87–3.18 (m, 5H), 3.40 (m, 1H), 4.47 (t, *J* = 8.2, 1H), 4.90 (q, *J* = 17.3, 2H), 7.58–7.62 (m, 2H), 7.83–8.00 (m, 4H). MS: *m*/*z* 292 (M^+, 48). Anal. ($C_{19}H_{20}N_2O\cdot 0.33\ H_2O$) C, H, N.

Compound (*S*)-**9g** was purified as a HCl salt by recrystallization from methanol–ethyl acetate (yield over two steps: 27%; mp 294–295 °C dec.); $[\alpha]_D^{24}$ +12.0° (*c* 0.5, methanol); $[\alpha]_D^{24}$ −42.6° (*c* 0.2, methanol–diethylamine 9:1). MS: *m*/*z* 292 (M^+, 43). Anal. ($C_{19}H_{20}N_2O\cdot HCl\cdot H_2O$) C, H, N.

X-ray crystallography

Single crystals of **7a**, **9a**, and **18** were submitted to X-ray data collection on a Siemens P4 four-circle diffractometer with graphite monochromated Mo-K_α radiation (λ = 0.71069 Å). The ω/2θ scan technique was used. The structures were solved by direct methods and the refinements were carried out by full-matrix anisotropic least-squares of F^2 against all reflections. The hydrogen atoms were located on Fourier difference maps and included in the structure-factor calculations with a common isotropic temperature factor. Atomic scattering factors including *f*′ and *f*″ were taken from ref 49. Structure solution and refinement were carried out by using the SHELX-97 package[49] while molecular graphics were performed by the SHELXTL PC program.[50]

7a. $C_{20}H_{22}N_2O$ (M_r 306.4), a single crystal, colorless needle, dimensions 0.6 × 0.2 × 0.2 mm, was used for data collection; monoclinic; space group $P2_1/c$ (no. 14); $a = 10.785$ (2), $b = 13.315$ (2), $c = 23.045$ (3) Å, ß = 98.18(1), $V = 3275.6$ (9) Å^3, $Z = 8$, $D_c = 1.24$ g/cm^3. A total of 5758 unique reflections ($R_{int} = 0.027$) was collected at 22 °C. The final refinement converged to $R = 0.056$ and $wR_2 = 0.099$ for $F^2 > 2\sigma(I)$. Minimum and maximum heights in last Δρ map were −0.19 and 0.17 eÅ^{-3}.

9a. $C_{20}H_{22}N_2O$ (M_r 306.4), a single crystal, colorless prism, dimensions 0.4 × 0.4 × 0.2 mm, was used for data collection; monoclinic; space group $P2_1/c$ (no. 14); $a = 14.433$ (2), $b = 12.476$ (2), $c = 9.673$ (1) Å, ß = 107.77 (1)°, $V = 1658.7$ (4) Å^3, $Z = 4$, $D_c = 1.23$ g/cm^3. A total of 2930 unique reflections ($R_{int} = 0.048$) were collected at 22 °C. The final refinement converged to $R = 0.050$ and $wR_2 = 0.096$ for $F^2 > 2\sigma(I)$. Minimum and maximum heights in last Δρ map were −0.17 and 0.15 eÅ^{-3}.

18. $C_{19}H_{25}N_3O$ (M_r 311.4), a single crystal, colorless prism, dimensions 0.3 × 0.3 × 0.2 mm, was used for data collection; monoclinic; space group $P2_1/c$ (no. 14); $a = 12.009$ (1), $b = 9.400$ (1), $c = 14.788$ (1) Å, ß = 94.37 (1)°, $V = 1664.5$ (3) Å^3, $Z = 4$, $D_c = 1.24$ g/cm^3. A total of 3818 unique reflections ($R_{int} = 0.025$) was collected at 22 °C. The final refinement converged to $R = 0.052$ and $wR_2 = 0.109$ for $F^2 > 2\sigma(I)$. Minimum and maximum heights in last Δρ map were −0.20 and 0.16 eÅ^{-3}.

Full crystallographic details will be given elsewhere.

Pharmacology

All experiments were carried out according to the Guide for the Care and Use of Laboratory Animals as adopted and promulgated by the US National Institutes of Health.

In vitro binding assays

Binding assays were performed as described in ref 30. Male Wistar rats (Charles River, Calco, Italy) were killed by decapitation, their brains were rapidly removed at 4 °C, and cortex and hippocampus were dissected out. Tissues were homogenized (Polytron PTA 10TS) in ice-cold Hepes buffer 50 mM, pH 7.4, and centrifuged according to the procedures indicated in the above-cited reference. The pellet obtained was finally suspended in Hepes buffer 50 mM, pH 7.4, just before the binding assay was performed. [^{3}H]Granisetron (s.a. 81 Ci/mmol; NEN Life Science Products) binding were assayed in final incubation volumes of 1 mL. Tissue and [^{3}H]ligand final concentration were 20 mg of tissue/sample and 0.5 nM, respectively. The specific binding of the tritiated ligand was defined as the difference between the binding in the absence (total binding) and in the presence of 100 μM unlabelled 5-HT (non-specific binding). It represented in an average 70% of the total binding.

Incubation was interrupted by rapid filtration under vacuum through Whatman GF/B glass fiber filters presoaked in Hepes buffer 50 mM, pH 7.4, containing 0.1% polyethyleneimine. Filters were immediately rinsed with

12 mL (3 × 4 mL) of ice-cold buffer by means of a Brandel M-24R cell harvester, dried and immersed into vials containing 8 mL of Ultima Gold MV (Packard Biosciences) for the measurement of trapped radioactivity with a TRI-CARB 1900TR (Packard Biosciences) liquid scintillation spectrometer, at a counting efficiency of about 60%. Competition experiments were analyzed by the 'Allfit' program[51] to obtain the concentration of unlabelled drug that caused 50% inhibition of [^{3}H]granisetron specific binding (IC_{50}). Apparent affinity constants (K_i) were derived from the IC_{50} values according to the Cheng and Prusoff equation.[52] The K_d value for [^{3}H]granisetron specific binding calculated from saturation isotherms was found to be 0.6 nM.

Measurement of [^{14}C]guanidinium uptake in NG 108-15 cells

This procedure has been described by Emerit et al.[35] Briefly, mouse neuroblastoma × rat glioma hybrid cells of the NG 108-15 clone were grown for 2 days in Dulbecco modified Eagle's medium supplemented with the appropriate nutrients.[35] The cell layer in each culture dish (35 mm) was then washed twice with 1.5 mL of buffer A (145 mM NaCl, 5.4 mM KCl, 1.8 mM $CaCl_2$, 1.0 mM $MgCl_2$, 2.0 mM Na_2HPO_4, 20 mM glucose, 20 mM Hepes, pH adjusted to 7.4 with NaOH), and covered with 1 mL of buffer B (same composition as buffer A except that [NaCl] was reduced to 135 mM and 10 mM guanidinium were added) containing 0.20–0.25 mCi of [^{14}C]guanidinium (s.a. 59 mCi/mmol, Service des Molécules Marquées at CEA, 91191 Gif-sur-Yvette, France), and, where indicated, 1 μM 5-HT, 10 μM substance P and/or eight different concentrations of each of the drugs to be tested. After 10 min at 37 °C, the assay was stopped by aspiration of the medium, and the cell layer was washed three times with 1.5 mL of ice-cold buffer C (same composition as buffer A except that NaCl was replaced by choline chloride). The cells were then dissolved into 0.5 mL of 0.4 M NaOH and the resulting extracts were transferred to scintillation vials. The culture dishes were further rinsed with 0.5 mL of 1 M HCl then 0.5 mL of 0.4 M NaOH, which were added to the vials. Each mixture (1.5 mL) was supplemented with 10 mL of the scintillation fluid Aquasol (New England Nuclear, Les Ulis, France) for radioactivity counting at 50% efficiency. All assays were performed in triplicate.

Under these conditions, [^{14}C]guanidinium accumulation in NG 108-15 cells was 2.5–3.5 times higher in the presence of both 1 μM 5-HT and 10 μM substance P than in their absence (basal uptake). 5-HT_3 receptor antagonists (zacopride, ondansetron, granisetron, tropisetron, etc.) completely prevented the stimulatory effect of 5-HT (with substance P) (see ref 35 for details).

Bezold–Jarisch reflex

The stimulation of cardiac 5-HT_3 receptors, in urethane-anaesthetized rats, is known to trigger a transient bradycardia known as the Bezold–Jarisch reflex. The ability of drugs to either induce or prevent this reflex has been used to further assess the 5-HT_3 receptor agonist or antagonist properties of the newly synthesized compounds. Briefly, adult male Sprague–Dawley rats (250–300 g body weight, Charles River, Calco, Italy) were anaesthetized with urethane (1.4 g/kg ip), and a tracheotomy was performed to insert an endotracheal tube. Blood pressure was recorded from carotid artery via a saline/heparin-filled pressure transducer, from which the heart rate was continuously monitored. Drugs were administered via the jugular vein. The Bezold–Jarisch reflex (which consists of a 50% drop in heart rate within 10–15 s following the injection of 30 μg/kg iv of serotonin) was assessed 5 and 15 min after the iv administration of various doses of each of the test compounds. Under these conditions, 10 mg/kg iv of either zacopride, ondansetron or tropisetron injected 5 min before 5-HT completely prevented the bradycardia normally evoked by the indoleamine.[37]

Nootropic activity

Nootropic activity was evaluated in mice by means of the passive avoidance test according to the method described by Jarvik and Kopp.[38] Briefly, the apparatus consisted of a two-compartment acrylic box with a lighted compartment connected to a darkened one by a guillotine door. On entering the dark compartment, the mice received a punishing electrical shock (0.5 mA, 1 s). The latency times for entering the dark compartment were measured in the training test and after 24 h in the retention test. Animals were injected with scopolamine to obtain memory disruption. The maximum entry latency allowed in the training session was 30 s, whereas in the retention session the entrance latency allowed was 120 s. The memory degree of received punishment was expressed as latencies recorded in the retention and training sessions.

Acknowledgements

Thanks are due to Italian MURST (ex 40% and ex 60% funds) and to French INSERM for financial support. M.C.M. and P.G.D.B. are especially grateful to Prof. Mati Karelson for the CODESSA Program and to CICAIA (Centro Interdipartimentale Calcolo Automatico e Informatica Applicata) for the Cerius2 program. Prof. Stefania D'Agata D'Ottavi's careful reading of the manuscript is also acknowledged. Unlabeled granisetron was a generous gift of Smith Kline Beecham Pharmaceuticals. The work was partially supported by the National Foundation of Cancer Research (NFCR).

References and Notes

1. Jackson, M. B.; Yakel, J. L. *Annu. Rev. Physiol.* **1995**, *57*, 447.
2. Boess, F. G.; Martin, I. L. *Neuropharmacology* **1994**, *33*, 275.
3. Wohland, T.; Friedrich, K.; Hovius, R.; Vogel, H. *Biochemistry* **1999**, *38*, 8671.
4. Unwin, N. *J. Mol. Biol.* **1993**, *229*, 1101.

5. Corringer, P.-J.; Le Novere, N.; Changeux, J.-P. *Annu. Rev. Pharmacol. Toxicol.* **2000**, *40*, 431.
6. Menziani, M. C.; De Rienzo, F.; Cappelli, A.; Anzini, M.; De Benedetti, P. G. A. *Theor. Chem. Acc.* **2001**, *106*, 98.
7. Silverstone, P. H.; Greenshaw, A. J. *Exp. Opin. Ther. Pat.* **1996**, *6*, 471.
8. (a) Cappelli, A.; Anzini, M.; Vomero, S.; Mennuni, L.; Makovec, F.; Doucet, E.; Hamon, M.; Bruni, G.; Romeo, M. R.; Menziani, M. C.; De Benedetti, P. G.; Langer, T. *J. Med. Chem.* **1998**, *41*, 728. (b) Cappelli, A.; Anzini, M.; Vomero, S.; Canullo, L.; Mennuni, L.; Makovec, F.; Doucet, E.; Hamon, M.; Menziani, M. C.; De Benedetti, P. G.; Bruni, G.; Romeo, M. R.; Giorgi, G.; Donati, A. *J. Med. Chem.* **1992**, *42*, 1556.
9. Clark, R. D.; Miller, A. B.; Berger, J.; Repke, D. B.; Weinhardt, K. K.; Kowalczyk, B. A.; Eglen, R. M.; Bonhaus, D. W.; Lee, C.-H.; Michel, A. D.; Smith, W. L.; Wong, E. H. F. *J. Med. Chem.* **1993**, *36*, 2645.
10. (a) Cappelli, A.; Donati, A.; Anzini, M.; Vomero, S.; De Benedetti, P. G.; Menziani, M. C.; Langer, T. *Bioorg. Med. Chem.* **1996**, *4*, 255. (b) Hibert, M. F.; Hoffmann, R.; Miller, R. C.; Carr, A. A. *J. Med. Chem.* **1990**, *33*, 1594.
11. (a) Menziani, M. C.; De Benedetti, P. G.; Karelson, M. *Bioorg. Med. Chem.* **1998**, *6*, 535. (b) Menziani, M. C.; Montorsi, M.; De Benedetti, P. G.; Karelson, M. *Bioorg. Med. Chem.* **1999**, *7*, 2437.
12. Archer, S.; Lewis, T. R.; Unser, M. J. *J. Am. Chem. Soc.* **1957**, *79*, 4194.
13. Mayer, F.; Sieglitz, A. *Chem. Ber.* **1922**, *55*, 1835.
14. Echavarren, A. M.; Stille, J. K. *J. Am. Chem. Soc.* **1987**, *109*, 5478.
15. Crisp, G. T.; Glink, P. T. *Tetrahedron* **1992**, *48*, 3541.
16. Lyle, R. E.; Portlock, D. E.; Kane, M. J.; Bristol, J. A. *J. Org. Chem.* **1972**, *37*, 3967.
17. Hayashi, H.; Miwa, Y.; Ichikawa, S.; Yoda, N.; Miki, I.; Ishii, A.; Kono, M.; Yasuzawa, T.; Suzuki, F. *J. Med. Chem.* **1993**, *36*, 617.
18. Anzini, M.; Cappelli, A.; Vomero, S.; Giorgi, G.; Langer, T.; Bruni, G.; Romeo, M. R.; Basile, A. S. *J. Med. Chem.* **1996**, *39*, 4275.
19. Quaternary allylammonium cations are allylating agents under Tsuji–Trost conditions, and the allyl group was employed for the protection of carboxylic acids, phoshoric acids, phenols, and amines; see: Garro-Helion, F.; Merzouk, A.; Guibé, F. *J. Org. Chem.* **1993**, *58*, 6109, and references cited therein.
20. The quaternary ammonium salt **43b** (intermediate of the synthesis of **8h**) was isolated and characterized by its ^{1}H NMR and mass spectra. ^{1}H NMR (DMSO-d_6): 2.01 (m, 3H), 2.23 (m, 1H), 2.47 (m, 1H), 3.48 (m, 3H), 3.64 (m, 1H), 3.87 (d, J=8.2, 2H), 3.97 (d, J=7.2, 2H), 4.66 (t, J=8.2, 1H), 4.89 (AB q, J=16.8, 2H), 5.55–5.63 (m, 2H), 5.93–6.14 (m, 1H), 7.68 (t, J=7.4, 1H), 7.89 (m, 1H), 8.10 (d, J=8.5, 1H), 8.21 (d, J=7.8, 1H), 8.79 (s, 1H). MS (FAB): m/z 334 (M^+, 14).
21. Shapiro, M. J.; Archinal, A. E.; Jarema, M. A. *J. Org. Chem.* **1989**, *54*, 5826.
22. Dewar, M. J. S.; Zoebisch, E. G.; Healey, E. F.; Stewart, J. J. P. *J. Am. Chem. Soc.* **1985**, *107*, 3902.
23. *Cerius2*. Molecular Simulations Inc.: San Diego, CA, 1997.
24. Montorsi, M.; Menziani, M. C.; Cocchi, M.; Fanelli, F.; De Benedetti, P. G. *Methods: Companion Meth. Enzymol.* **1998**, 239.
25. Cocchi, M.; De Benedetti, P. G. *J. Mol. Model* **1998**, *4*, 113.
26. *QUANTA/CHARMm*. Molecular Simulations Inc.: 16 New England Executive Park, Burlington, MA 01803-5297, USA, 1996.
27. Katritzky, A. R.; Lobanov, V. S.; Karelson, M. *Chem. Soc. Rev.* **1995**, 279.
28. Katritzky, A. R.; Mu, L.; Lobanov, V. S.; Karelson, M. *J. Phys. Chem.* **1996**, *100*, 10400.
29. Brooks, B. R.; Bruccoleri, R. E.; Olafson, B. D.; States, D. J.; Swaminathan, S.; Karplus, M. *J. Comput. Chem.* **1983**, *4*, 187.
30. Nelson, D. R.; Thomas, D. R. *Biochem. Pharmacol.* **1989**, *38*, 1693.
31. Stanton, D. T.; Jurs, P. C. *Anal. Chem.* **1990**, *62*, 2323.
32. Kier, L. B. *J. Pharm. Sci.* **1980**, *69*, 807.
33. Papineni, R. V. L.; Pedersen, E. *J. Biol. Chem.* **1997**, *272*, 24891.
34. Ohno, K.; Wang, H. L.; Milone, M.; Bren, N.; Brengman, J.; Nakano, S.; Quiram, P.; Pruitt, J.; Sine, S. M.; Engel, A. *Neuron.* **1996**, *17*, 157.
35. Emerit, M. B.; Riad, M.; Fattaccini, C. M.; Hamon, M. *J. Neurochem.* **1993**, *60*, 2059.
36. Bolanos, F. J.; Schechter, L. E.; Miquel, M. C.; Emerit, M. B.; Rumigny, J. F.; Hamon, M.; Gozlan, H. *Biochem. Pharmacol.* **1990**, *40*, 1541.
37. Cohen, M. L.; Bloomquist, W.; Gidda, J. S.; Lacefield, W. *J. Pharmacol. Exp. Ther.* **1989**, *248*, 197.
38. Jarvik, M. E.; Kopp, R. *Psychol. Rep.* **1967**, *21*, 221.
39. Gaster, L. M.; King, F. D. *Med. Res. Rev.* **1997**, *17*, 163.
40. Langlois, M.; Soulier, J. L.; Rampillon, V.; Gallais, C.; Brémont, B.; Shen, S.; Yang, D.; Giudice, A.; Sureau, F. *Eur. J. Med. Chem.* **1994**, *29*, 925.
41. Clark, R. D.; Muchowski, J. M.; Weinhardt, K. K.; Dillon, M. P.; Lee, C.-H.; Bley, K. R.; Bonhaus, D. W.; Wong, E. H. F.; Eglen, R. M. *Bioorg. Med. Chem. Lett.* **1995**, *5*, 1853.
42. Karlin, A.; Akabas, M. H. *Neuron.* **1995**, *15*, 1231, and references cited therein.
43. Meltzer, P. C.; Liang, A. Y.; Brownell, A.-L.; Elmaleh, D. R.; Madras, B. K. *J. Med. Chem.* **1993**, *36*, 855.
44. Rigaudy, J.; Maumy, M. *Bull. Soc. Chim. Fr.* **1972**, 3936.
45. Maeyama, K.; Iwasawa, N. *J. Org. Chem.* **1999**, *64*, 1344.
46. Ornstein, G. *Chem. Ber.* **1907**, *40*, 1088.
47. Canonne, P.; Boulanger, R.; Bernatchez, M. *Tetrahedron* **1989**, *45*, 2525.
48. Powers, J. C.; Ponticello, I. *J. Am. Chem. Soc.* **1968**, *90*, 7102.
49. Sheldrick, G. M. *SHELX-97, Rel. 97-2, Program for X-ray Data Diffraction*. Gottingen University, 1997.
50. *SHELXTL PC, Ver. 5*. Siemens Industrial Automation Inc.: Madison, WI, 1994.
51. De Lean, K. W.; Munson, P. J.; Rodbard, D. *Am. J. Physiol.* **1978**, *235*, E97.
52. Cheng, Y.; Prusoff, W. H. *Biochem. Pharmacol.* **1973**, *22*, 3099.